THE THERMAL NEUTRON CAPTURE CROSS SECTIONS OF SOME REACTOR-PRODUCED RADIONUCLIDES

by

MYRON F. ELGART

A dissertation submitted to the Graduate Faculty in Chemistry in partial fulfillment of the requirements for the degree of Doctor of Philosophy.

The City University of New York

1971

This manuscript has been read and accepted for the Graduate Faculty in Chemistry in satisfaction of the dissertation requirement for the degree of Doctor of Philosophy.

May 17, 1971
date

Chairman of Examining Committee

May 18 1971
date

Executive Officer

Supervisory Committee

The City University of New York

PLEASE NOTE:

Some Pages have indistinct print. Filmed as received.

UNIVERSITY MICROFILMS

Abstract

THE THERMAL NEUTRON CAPTURE CROSS SECTIONS

OF SOME REACTOR-PRODUCED RADIONUCLIDES

by

Myron F. Elgart

Advisers: Professor Harmon L. Finston

Professor Evan T. Williams

A technique has been developed for the determination of thermal neutron capture cross sections of radioactive nuclides. The simultaneous production, decay and burnup of a radioactive nuclide in the core of a nuclear reactor has been studied. The Westcott formalism, which is based on the technique of activation, has been applied to this burnup technique, with the following results:

I^{126} $\hat{\sigma}$ = 20000 barns

σ_o = 5960 barns

RI = 40600 barns

Sb^{124} $\hat{\sigma}$ = 6290 barns

σ_o = 2990 barns

RI = 10200 barns

Co^{58} $\hat{\sigma}$ = 4480 barns

σ_o = 2310 barns

RI = 6890 barns

Results for I^{126} have not been previously reported. The results

for Sb^{124} have determined the westcott parameters for this nuclide, which were previously in doubt. The results for Co^{58} show that previous work using this nuclide as a measure of the fast neutron flux are in error.

ACKNOWLEDGEMENTS

The author wishes to make the following acknowledgements:

To H.L. Finston, who led the way.

To E.T. Williams, who pulled when others pushed.

To T. Ishida, who will finally get his own work done.

To L. Reiss, O. Safferling, J. Gavlick, S. Wacks, J.J. Floyd and J. Stehn, whose contributions made this work possible.

To E. Yellin, who stayed one afternoon to talk.

And to Annette, whose patience was indeed a virtue.

It is the author's wish to dedicate this thesis to his mother.

TABLE OF CONTENTS

LIST OF TABLES

LIST OF FIGURES

I. Introduction

The determination of thermal neutron capture cross sections (tnccs) is of fundamental importance for nuclear theory, nuclear applications and reactor technology. Although tnccs of stable nuclei have been intensively studied, data for the tnccs of radioactive nuclei are rarely found in the literature. These data have always been difficult to obtain experimentally. The various techniques used, such as activation, burnup and mass spectrometry, do not always yield consistent values.

A. Reactor considerations

The importance of tnccs for the quantitative evaluation of the changes in reactivity which occur in a nuclear reactor during operation has directed considerable effort towards their determination. Consequently, most work on the tnccs of radioactive nuclei has involved the fission products. Cross sections of some of these nuclei are crucially important in the calculation of the effective multiplication factor, k, which is one of the major parameters used in reactor design theory[1]. The parameter k represents the number of second generation fissions in U^{235} per fission of U^{235} by a first generation neutron.

The reactivity of a nuclear reactor is defined as[2]

$$\text{Reactivity} = (k - 1) / k. \qquad (1)$$

When k = 1, the reactivity is zero and the reactor is operating in a steady-state condition. However, to initiate the chain

reaction ("start up" of the reactor) or to increase the power output, k must be greater than one to make the reactivity greater than zero. For a medium of infinite extent, the multiplication factor reduces to the expression[3]

$$k_\infty = \frac{\nu \sigma_f N_f}{\sigma_f N_f + \sum_i \sigma_{c,i} N_i} \qquad (2)$$

where: ν = number of neutrons emitted per fission

σ_f = macroscopic fission cross section

N_f = number of fissionable nuclei per cm^3

$\sigma_{c,i}$ = capture cross section of the i^{th} nuclide

N_i = number of nuclei of the i^{th} nuclide per cm^3.

Equation (2) is valid for monoenergetic thermal neutrons (the velocity of a thermal neutron is 2200 m / sec). However, neutrons in a reactor are not monoenergetic. Since capture cross sections vary with the energy of the incident neutron, the expression for k_∞ (equation (2)) must be averaged over the neutron energy spectrum to calculate the number of neutrons produced per thermal neutron absorbed.

B. Xenon-135

The phenomenon known as xenon poisoning clearly illustrates the need for accurate values of the tnccs for certain fission products. The nuclide Xe^{135} ($t_{\frac{1}{2}}$ = 9.2 hr) is formed primarily by the decay of I^{135} ($t_{\frac{1}{2}}$ = 6.7 hr). Xenon-135 is of interest both theoretically and practically, since it is formed in fission in relatively high yield. Its tnccs approaches the maximum theoretical

value[4],

$$\sigma_{reaction} = \pi \lambda^2, \tag{3}$$

where equation (3) is valid for reactions of thermal neutrons (ℓ=0). Since the tnccs of Xe^{135} is orders of magnitude greater than most cross sections, this nuclide is extremely important in reactor technology.

In steady-state operation of a reactor, such as the Materials Testing Reactor (MTR) at the National Reactor Testing Station in Idaho, k is reduced by about 0.04 due to the presence of Xe^{135}. If the MTR is shut down for a few minutes after a period of steady-state operation, the concentration of Xe^{135} increases (Xe^{135} is no longer consumed by the Xe^{135} (n,γ) Xe^{136} reaction but is still produced by the decay of I^{135}) to the point where, about twenty minutes after shutdown, the MTR cannot be started up again. The Xe^{135} concentration reaches a maximum value about ten hours after shutdown, reducing k to a value of about 0.7. The MTR reaches critical condition again (k=1) after a wait of about two days, when most of the Xe^{135} has decayed.

Petruska et al.[5] measured both fission yield and tnccs of Xe^{135}, using mass spectrometric techniques. Two samples of natural uranium were irradiated in the N.R.X. reactor at Chalk River in different positions, thus exposing the uranium samples to different thermal neutron fluxes. The fission yields in both samples for Cs^{133}, Cs^{135} and Cs^{137} were determined with a mass spectrometer. The nuclide Xe^{135} decays by beta emission to Cs^{135} or undergoes the Xe^{135} (n,γ) Xe^{136} burnup reaction. The decrease

in fission yield of Cs^{135} with increased thermal neutron flux can be attributed to the Xe^{135} burnup reaction. A knowledge of the changes in the thermal flux and the fission yield for the two uranium samples enabled the authors to calculate a value for the effective cross section of Xe^{135}, $\sigma = 3.47 \times 10^6$ barns, assuming that the tnccs of Xe^{135} follows the 1/v law.

In 1956, S. Bernstein et al.[6] reported some work done in 1948 at Oak Ridge National Laboratory concerning the variation of the capture cross section of Xe^{135} with incident neutron energy. The variation of this cross section is an important parameter in the design of nuclear reactors which could be operated at various neutron temperatures. Fission product iodine was separated from irradiated uranium metal and precipitated as palladium iodide. All chemical processes were performed in a concrete hot cell by remote control because the activity of the fission products amounted to several thousand curies. A crystal spectrometer was used to determine neutron energy. Iodine-135, in the form of palladium iodide, was allowed to decay to Xe^{135}. Neutron transmission measurements were made on the samples of xenon produced. The total cross section for neutrons below an energy of 0.55 ev (this corresponds to the cadmium cut-off energy, i.e. neutrons with energy less than 0.6 ev are effectively absorbed by cadmium) corresponding to a neutron temperature of 520° K, was reported to be 2.6×10^6 barns.

M.S. Freedman et al.[7] employed two different techniques to determine the tnccs of Xe^{135}. The first method, proposed by E. Wigner, consisted of the irradiation of two uranium samples

in different thermal neutron fluxes to give different amounts of Xe^{135}. The equation

$$FY = (\lambda + \sigma_c \phi)N \ , \tag{4}$$

where: F = fission rate

Y = fission yield

λ = decay constant of Xe^{135}

σ_c = capture cross section of Xe^{135}

ϕ = thermal neutron flux

N = number of Xe^{135} atoms produced,

was used to determine the capture cross section of Xe^{135}. This method, with its inherent experimental difficulties in determining the thermal flux and in removing Xe^{135} from the uranium after irradiation (to prevent changes in the Xe^{135} activity due to the decay of I^{135}), gave the value of $2.36 \pm 0.59 \times 10^6$ barns for the capture cross section of Xe^{135}.

The second technique used was suggested by N. Elliot and coworkers. A sample of Xe^{135} was used to make two samples, each sample having approximately one-half of the original Xe^{135} activity. One of the samples was then irradiated in a flux of thermal neutrons. For the sample of Xe^{135} which was irradiated,

$$A' = A'_o e^{-(\lambda + \sigma_c \phi)t} \tag{5}$$

where: A'_o = initial activity of Xe^{135}

A' = activity of Xe^{135} after irradiation.

For the sample of Xe^{135} which was not irradiated,

$$A = A_o e^{-\lambda t}. \tag{6}$$

Division of equation (6) by equation (5) gives

$$\frac{A}{A'} = \frac{A_o}{A'_o} \exp[\sigma_c \phi t] \tag{7}$$

Equation (7) is solved for σ_c to give

$$\sigma_c = \frac{\ln[A/A' \times A'_o/A_o]}{\phi t} \tag{8}$$

The ratio of Xe^{135} activity in the irradiated sample to the Xe^{135} activity in the unirradiated sample could be varied by changing the time of irradiation. An average of four experiments of this type gave a value of $\sigma_c = 2.58 \pm 0.2$ barns ($T = 400^oK$) for Xe^{135}. The most serious experimental difficulty was due to the fact that 50% of the total xenon activity was due to Xe^{133}.

Fickel and Tomlinson[8] determined the tnccs of Xe^{135} by mass spectrometric techniques. Since Cs^{135} is formed by the decay of Xe^{135}, the amount of Cs^{135} present in the fission products is dependent on the tnccs of Xe^{135}. Samples of U^{235} were irradiated, using cobalt flux monitors to determine the thermal neutron flux. The calculation of the results followed the procedures of Petruska et al.[5] The values obtained were $\sigma_c = 3.15 \pm 0.06 \times 10^6$ barns ($T = 120^oC$) and $\sigma_c = 3.27 \pm 0.11$ barns ($T = 137^oC$).

C. Other fission products

An activation technique was used by Sugarman[9] to determine the tnccs of Cs^{135}. Fission product Xe^{135} was collected and allowed to decay to Cs^{135}. This sample was then irradiated with thermal neutrons. The resulting activity of Cs^{136} was measured

and the tnccs was determined to be 14.5 ± 4.4 barns.

Baerg et al.[10] separated cesium from the fission products of irradiated uranium metal. The Cs^{135}/Cs^{137} ratio was measured with a mass spectrometer. The cesium sample was then irradiated with thermal neutrons. The Cs^{136}/Cs^{137} ratio was determined by beta-counting. The Cs^{135}/Cs^{137} ratio was redetermined with a mass spectrometer. The Cs^{136}/Cs^{135} ratio could then be deduced and a tnccs of 8.7 ± 0.5 barns for Cs^{135} was calculated.

Cross sections for the fission products in the rare earth region were investigated by Inghram et al.[11] A thick uranium slug was irradiated for three years to obtain the fission products. Mass spectrometric techniques, using isotope dilution methods, were used to determine the ratios of various nuclides. Comparison of the measured ratios with ratios calculated on the basis of theoretical fission yields enabled the authors to calculate the tnccs of these nuclides. The nuclide Gd^{157} was reported to have a tnccs of 5.95×10^4 barns. This value differed considerably from previously reported results[12,13] of 2×10^5 barns.

Kennett and Thode [14] investigated the absorption cross sections of several fission products obtained from the irradiation of plutonium. Mass spectrometric techniques were used to determine the cross sections for Kr^{83}, I^{131} and Xe^{133}. The absorption cross sections were reported to be 216 ± 43 barns for Kr^{83} (as compared to 205 ± 10 barns[15]), 51 ± 41 barns for I^{131} (as compared to 600 ± 300 barns[16]), and 188 ± 89 barns for Xe^{133} (as compared to an upper limit of 3000 barns[17]).

A final example of the determination of tnccs for the fission

products is the study of the tnccs of Pr^{143} by Roy and Roy[18]. A short thermal neutron irradiation of Ce^{142} produced Ce^{143}, which decayed to Pr^{143}. The samples of Pr^{143} were then irradiated with thermal neutrons to produce Pr^{144}. The decay of this sample was followed by beta-particle counting with an absorber interposed which stopped the beta particles from Pr^{143} (E_β = 0.77 MeV) but not those from Pr^{144} (E_β = 3 MeV). The decay curves were then resolved into a Pr^{144} component and a background component. The results were reported, following the Westcott convention[19] (to be discussed later), to be σ_o = 89 ± 10 barns and $\hat{\sigma}$ = 93 ± 10 barns.

D. Iodine-126

Many radioactive nuclides have no reported cross sections, usually because suitable quantities cannot be obtained for experimental use. For instance, there is no reported cross section for I^{126}, even though sufficient research[20-26] has been done on this nuclide to characterize its half-life and decay scheme.

E. The burnup technique

Although some cross sections for radioactive nuclides have been obtained by mass spectrometric techniques, most are obtained by activation or burnup techniques. The cross section for I^{126} could not be obtained by activation with thermal neutrons because the product nuclide, I^{127}, is not radioactive. In a burnup experiment a radioactive nuclide is destroyed by reaction with thermal neutrons. The differential equation for this process is

$$-\frac{dN}{dt} = \lambda N + \sigma_T \phi_T N \ , \qquad (9)$$

where: N = number of radioactive nuclei

t = time of irradiation

λ = decay constant

σ_T = thermal neutron capture cross section

ϕ_T = thermal neutron flux.

Equation (9) can be integrated from $N = N_o$ at $t = 0$ to $N = N$ at $t = t$ and solved for σ_T to give

$$\sigma_T = \frac{1}{\phi_T t} \ln[N_o/N] - \frac{\lambda}{\phi_T} \ . \qquad (10)$$

The thermal neutron capture cross section is determined by the decrease of activity associated with the burnup reaction.

Roy and Wuschke[27] and Bresesti et al.[28] have measured the cross section for several isotopes of iodine by means of the burnup technique. The major experimental problem associated with these evaluations of capture cross sections was that of obtaining sufficient quantities of the various radioactive isotopes in reasonably pure form. The capture cross section of Sb^{124} was determined by Eastwood and Brown[29] and by Murin et al.[30], with disparate results of less than 20 barns[29] and 2000 barns[30]. The diversity of these results reflects the experimental difficulties inherent in the burnup technique.

The tnccs of Na^{22} has been reported variously as 90000 barns, 35900 barns and 6000 barns. These results have been tabulated in reference (31). The cross section for this nuclide is an important parameter in calculating the operating characteristics for sodium-cooled reactors. The discrepancy points out the diffi-

culty in obtaining these important data.

F. Cobalt-58

The reaction $Ni^{58}(n,p)Co^{58}$ is used routinely as a fast-neutron flux monitor. However, it was found[32] that the fast-neutron flux determined by nickel monitors varied according to the irradiation period. This phenomenon could by explained by a burnup of the 71.3 day Co^{58} isomer produced by the reactions of fast neutrons with Ni^{58} if the tnccs of this isomer was large. Thus, it is necessary to carefully measure this cross section so that correction factors for the irradiation period and the thermal neutron flux can be determined when using nickel as a fast-flux monitor. The capture cross section of 71.3 day Co^{58} has been reported to be 1650 barns[32] and 3750 barns[33]. These values are large enough to produce the observed effect, and the discrepency in the reported values will seriously affect the calculation of the correction factors. The tnccs of the 9.3 hour Co^{58m} isomer was reported to be 140000 barns[32].

II. Theoretical Considerations

A. Neutron interactions

Neutrons interact with nuclei in a variety of ways. For an elastic collision, where only scattering of the neutron takes place,

$$n + Z^A \rightarrow Z^A + n \ , \tag{11}$$

there is no net change of total kinetic energy. Transfer of energy between the incident neutron and the target nucleus may take place, however,

$$n + Z^A \rightarrow (Z^A)^* + n' \ , \tag{12}$$

and this process is known as inelastic scattering. The target nucleus is left in an excited state, and the two particles re-emerge with total kinetic energy lower than its initial value by the amount of energy spent to excite the nucleus. A thermal neutron (with the average energy of 0.025 eV, corresponding to a neutron velocity of 2200 m/sec) can be absorbed by the target nucleus, so that

$$n + Z^A \rightarrow Z^{A+1} + \gamma \ . \tag{13}$$

This reaction is known as the radiative capture process and is the predominant nuclear reaction for thermal neutrons.

At higher neutron energies, other nuclear reactions, such as

$$n + Z^A \rightarrow (Z-1)^A + p \ , \tag{14}$$

$$n + Z^A \rightarrow (Z-2)^{A-3} + \alpha \ , \tag{15}$$

$$n + Z^A \rightarrow Z^{A-1} + 2n \ , \tag{16}$$

can take place. These reactions tend to predominate at higher incident neutron energies.

The cross section of a nucleus is known to vary with the energy of the incident neutron (in the low-energy region). This problem in compound-nucleus theory was first solved by Breit and Wigner[34]. For the (n,γ) reaction (the radiative capture process), the Breit-Wigner one-level formula for the variation of the cross section with neutron energy is[35]

$$\sigma_{(n,\gamma)} = \pi\lambda^2 \frac{2I_C + 1}{2(2I_A + 1)} \frac{\Gamma_n\Gamma_\gamma}{(\epsilon-\epsilon_o)^2 + (\Gamma/2)^2} \qquad (17)$$

where:

I_C = spin of the compound nucleus

I_A = spin of the target nucleus

Γ_n = partial width for neutron emission

Γ_γ = partial width for gamma emission

ϵ_o = energy at which resonance occurs

Γ = total width of the level.

The cross section will show maxima when $\epsilon=\epsilon_o$. Thus, depending on the target nuclide, the capture of neutrons in the resonance region may also be an important reaction. Resonance capture occurs generally in the neutron energy range of several eV to several hundreds of eV.

Significant production of radioactive nuclides by reactions (14), (15) and (16) requires a high flux of sufficiently energetic neutrons. A suitable flux is available in the core of a reactor such as the high-flux beam reactor (HFBR) at Brookhaven National Laboratory. Burnup of product nuclei by neutrons in the thermal

and resonance energy regions will also occur to an appreciable extent in the core of this reactor.

B. The basic problem

The differential equation for the production of a radioactive nuclide undergoing these reactions is

$$\frac{dN}{dt} = \sigma_P \phi_P N_P - \lambda N - \sigma_T \phi_T N - \sigma_R \phi_R N \qquad (18)$$

where: N_P = number of target nuclei

σ_P = cross section for the production of the radioactive product nucleus by reactions (14), (15) or (16)

ϕ_P = epithreshold flux for production

λ = decay constant for the radioactive product

N = number of radioactive nuclei produced

subscript T refers to burnup by thermal neutron capture

subscript R refers to burnup by resonance neutron capture.

An order-of-magnitude calculation[36] for the number of target nuclei consumed by undergoing reaction during the irradiation indicated that N_P could be assumed constant for the nuclides under consideration. Equation (18) can now be integrated from N=0 at t(irradiation)=0 to $N=N_B$ at t(irradiation)=t to give

$$N_B = \frac{\sigma_P \phi_P N_P (1 - e^{-[\lambda + \sigma_T \phi_T + \sigma_R \phi_R]t})}{\lambda + \sigma_T \phi_T + \sigma_R \phi_R} \qquad (19)$$

where: subscript B refers to an unshielded (bare) sample.

If the target nuclide was placed in a cadmium shield, the thermal neutron burnup would be diminished by a factor k, where

$$k = \frac{\phi_T \text{ inside the cadmium shield}}{\phi_T \text{ outside the cadmium shield}} . \qquad (20)$$

The differential equation for the production of a radioactive nuclide inside a cadmium shield is

$$\frac{dN}{dt} = \sigma_P \phi_P N_P - \lambda N - k\sigma_T \phi_T N - \sigma_R \phi_R N . \qquad (21)$$

Equation (21) can be integrated from N=0 at t(irradiation)=0 to $N=N_{Cd}$ at t(irradiation)=t to give

$$N_{Cd} = \frac{\sigma_P \phi_P N_P \left(1 - e^{-[\lambda + k\sigma_T \phi_T + \sigma_R \phi_R]t}\right)}{\lambda + k\sigma_T \phi_T + \sigma_R \phi_R} \qquad (22)$$

where: subscript Cd refers to a cadmium-covered sample.

By dividing equation (22) by equation (19), an expression is obtained which is independent of the production rate:

$$\frac{N_{Cd}}{N_B} = \frac{\left(1 - e^{-[\lambda + k\sigma_T \phi_T + \sigma_R \phi_R]t}\right)(\lambda + \sigma_T \phi_T + \sigma_R \phi_R)}{\left(1 - e^{-[\lambda + \sigma_T \phi_T + \sigma_R \phi_R]t}\right)(\lambda + k\sigma_T \phi_T + \sigma_R \phi_R)} . \qquad (23)$$

The $Co^{59}(n,\gamma)Co^{60}$ reaction is commonly used as a thermal flux monitor. The differential equation representing the formation of Co^{60} in a reactor is

$$\frac{dN}{dt} = \sigma_T \phi_T N_o + \sigma_R \phi_R N_o - \lambda N - (\text{burnup}) , \qquad (24)$$

where: N_o = number of Co^{59} nuclei.

If the time of irradiation is much less than the halflife of Co^{60} and $\sigma_T + \sigma_R$ is small for Co^{60}, the last two terms of equation (24)

can be neglected, and equation (24) can be integrated to give

$$N_B = (\sigma_T \phi_T + \sigma_R \phi_R) N_o t \ . \tag{25}$$

In a similar manner, irradiation of Co^{59} inside a cadmium shield can be described by the expression

$$N_{Cd} = (k\sigma_T \phi_T + \sigma_R \phi_R) N_o t \ . \tag{26}$$

If equation (26) is subtracted from equation (25), an expression for k can be derived:

$$1 - k = \frac{N_B - N_{Cd}}{\sigma_T \phi_T N_o t} \ . \tag{27}$$

In the usual case of irradiation in thermal neutron beams or in well-thermalized reactor positions, resonance absorption is neglected and the value for k is usually obtained by dividing equation (26) by equation (25) to get

$$k = \frac{N_{Cd}}{N_B} \ . \tag{28}$$

C. The Westcott formalism

Consideration of equations (27) and (28) indicates that, unless the thermal neutron flux is much greater than the resonance neutron flux, resonance absorption cannot be neglected. The contribution of this term makes determination of the thermal neutron flux by cobalt activation more difficult. Thus, while cross sections for neutrons at a single energy can be determined unambiguously, considerable difficulty can be encountered in the definition of effective cross sections in various reactors having

different neutron spectra.

In 1957 Westcott et al.[19] published a procedure, then in use at Chalk River, for the determination of the thermal flux and the tnccs of a nuclide which allowed intercomparison of results obtained in different nuclear reactors in a clearly defined manner. This convention is now used universally for reactor experiments.

The effective cross section for a target nucleus, $\hat{\sigma}$, is defined by equating the reaction rate per atom present per second, R, to the product of $\hat{\sigma}$ with nv_o,

$$R = \hat{\sigma} n v_o \tag{29}$$

where: n = the neutron density, including both thermal and epithermal neutrons

v_o = 2200 m/sec.

In this convention, the quantity nv_o corresponds to the flux. The term "2200 m/sec flux" is used to distinguish nv_o from other quantities used as measures of the neutron flux.

In the Westcott convention, the neutron spectrum is divided into two parts; the Maxwellian distribution of thermal neutrons corresponding to the average temperature T°K, and the epithermal 1/E flux distribution, cut off at a suitable lower limit of energy. The cross section is corrected for its deviation from the 1/v law. The relative contribution of the epithermal 1/E component is also taken into account. The effective cross section is therefore defined as

$$\hat{\sigma} = \sigma_o(g + rs) \tag{30}$$

where: σ_o = cross section for 2200 m/sec neutrons

r = epithermal index

g,s = correction factors for the deviation of the cross section from the 1/v law in the thermal and epithermal regions, respectively.

For a 1/v absorber, such as lithium or boron, the effective absorption cross section is simply the value at 2200 m/sec, and g=1 and s=0 for these nuclides.

Since reactor neutron temperatures are not usually measured, it is convenient to use a temperature-independent term for s, so that

$$s_o = s(T_o/T)^{\frac{1}{2}} . \tag{31}$$

The epithermal index can now be obtained experimentally by using the expression[37]

$$r(T/T_o)^{\frac{1}{2}} = \frac{1}{R_{Cd}(s_o + 1/K) - s_o} \tag{32}$$

where: R_{Cd} = ratio of the rate of the $Co^{59}(n,\gamma)Co^{60}$ reaction of a bare monitor to the rate under a cadmium filter.

K = a coefficient calculated from the variation of the cadmium cross section with neutron energy and the thickness of cadmium used.

Values of K for various thicknesses of cadmium have been tabulated in reference (19).

The cadmium ratio and the rate of reaction can be determined experimentally for cobalt flux monitors. Equations (32) and (30) are used to determine $\hat{\phi}_o$. The 2200 m/sec flux is now determined from equation (29).

The Westcott convention is used to determine the various nuclear parameters for a nuclide undergoing irradiation using

cobalt monitors. The induced activity is measured in bare and cadmium-covered samples to obtain the cadmium ratio, which is defined as

$$R_{Cd} = \frac{R \text{ in bare sample}}{R \text{ in cadmium-covered sample}} . \tag{33}$$

Equation (32) is solved for s_o to give

$$s_o = \frac{1}{R_{Cd} - 1} \left[\frac{1}{r}\left(\frac{T_o}{T}\right)^{\frac{1}{2}} - \frac{R_{Cd}}{K}\right] . \tag{34}$$

The value of s_o for the target nuclide can now be obtained from equation (34). Assuming that g=1, a value for σ_o can now be obtained from equation (30), where $\hat{\sigma}$ has been obtained from equation (29).

The resonance integral (RI) of the target nuclide is the total capture cross section with a suitable lower energy limit, and is usually defined as

$$RI = \int_{0.6\ eV}^{E(fission)} \sigma_c(E)\,dE/E . \tag{35}$$

The resonance integral of the target nuclide can be experimentally determined from the relationship[37]

$$RI_x = RI_{Co} \frac{(R_{Cd} - 1)_{Co}\ \sigma_{o,x}}{(R_{Cd} - 1)_x\ \sigma_{o,Co}} , \tag{36}$$

where: subscript Co refers to the cobalt monitors

subscript X refers to the target nucleus.

D. Application of the Westcott formalism to the problem of interest

We now apply the Westcott convention to the case of any nuclide, radioactive or stable, in the core of the HFBR. The differential equation representing the production of a radioactive nuclide becomes

$$\frac{dN}{dt} = \sigma_P \phi_P N_P - \lambda N - \hat{\sigma} n v_o N \ . \tag{37}$$

Equation (37) can be integrated from N=0 at t(irradiation)=0 to $N=N_B$ at t(irradiation)=t, leading to

$$N_B = \frac{\sigma_P \phi_P N_P \ (1 - e^{-[\lambda + \hat{\sigma} n v_o]t})}{\lambda + \hat{\sigma} n v_o} \ . \tag{38}$$

The differential equation representing the production of a radioactive nuclide under a cadmium shield is

$$\frac{dN}{dt} = \sigma_P \phi_P N_P - \lambda N - k\hat{\sigma} n v_o N \ . \tag{39}$$

This equation, when integrated from N=0 at t(irradiation)=0 to $N=N_{Cd}$ at t(irradiation)=t, gives

$$N_{Cd} = \frac{\sigma_P \phi_P N_P \ (1 - e^{-[\lambda + k\hat{\sigma} n v_o]t})}{\lambda + k\hat{\sigma} n v_o} \ . \tag{40}$$

Equation (40) is divided by equation (38) to give

$$\frac{N_{Cd}}{N_B} = \frac{(1 - e^{-[\lambda + k\hat{\sigma} n v_o]t}) \ (\lambda + \hat{\sigma} n v_o)}{(1 - e^{-[\lambda + \hat{\sigma} n v_o]t}) \ (\lambda + k\hat{\sigma} n v_o)} \ . \tag{41}$$

Equation (41) is a transcendental equation in terms of $\hat{\sigma}$, the

effective cross section. Therefore, $\hat{\sigma}$ is determined by numerical solution of equation (41).

The Westcott convention is based on results of an activation experiment, but the previous equations have been concerned with burnup. The use of the Westcott formalism requires the knowledge of the number of nuclei produced from burnup. Thus, the cadmium ratio can be defined as

$$R_{Cd} = \frac{N_{total} - N_B}{N_{total} - N_{Cd}} \tag{42}$$

where: N_{total} = total number of radioactive nuclei produced.

Although the total number of product nuclei is not known, the ratio of the total number of product nuclei in the bare sample to the number of product nuclei found experimentally in the bare sample can be determined from the relationship –

$$\frac{N_{total}}{N_B} = \frac{(1 - e^{-\lambda t})\ (\lambda + \hat{\sigma} n v_o)}{(1 - e^{-[\lambda + \hat{\sigma} n v_o]t})\ (\lambda)} . \tag{43}$$

In the derivation of equation (43), the total number of product nuclei, N_{total}, is the number of nuclei which would have been formed if no burnup occurred. This is analagous to shielding a sample from all of the nv_o flux, i.e. k=0. The differential equation for the case when k=0 is

$$\frac{dN}{dt} = \sigma_P \phi_P N_P - \lambda N . \tag{44}$$

Equation (44) can be integrated from N=0 at t(irradiation)=0 to $N=N_{total}$ at t(irradiation)=t to give

$$N_{total} = \frac{\sigma_P \phi_P N_P \ (1 - e^{-\lambda t})}{\lambda} \ . \tag{45}$$

If equation (45) is divided by equation (38), equation (43) is deduced. Since σ can be obtained from equation (41), N_{total}/N_B of equation (43) can be evaluated.

In order to apply the Westcott convention, it is necessary to know the number of product nuclei from activation, N_{act}, where

$$N_{B,act} = N_{total} - N_B \ , \tag{46}$$

for the bare sample, and

$$N_{Cd,act} = N_{total} - N_{Cd} \tag{47}$$

for the cadmium-covered sample. Equations (46) and (47) are now divided by N_B to give

$$\frac{N_{B,act}}{N_B} = \frac{N_{total}}{N_{Cd}} - 1 \tag{48}$$

and

$$\frac{N_{Cd,act}}{N_B} = \frac{N_{total}}{N_B} - \frac{N_{Cd}}{N_B} \ , \tag{49}$$

respectively. Equation (48) is divided by equation (49) to give

$$\frac{N_{B,act}}{N_{Cd,act}} = \frac{N_{total}/N_B - 1}{N_{total}/N_B - N_{Cd}/N_B} \ , \tag{50}$$

which is another form of equation (42). The ratio N_{Cd}/N_B is determined experimentally. The ratio N_{total}/N_B is determined from equation (43). Thus, equation (50) can be solved to give R_{Cd} in the sense of the Westcott formalism.

Once R_{Cd} has been determined, σ_o and RI can be determined

for the radioactive product nuclide by following the procedures of the Westcott convention.

III. Experimental Procedures

A preliminary experiment was performed in this laboratory several years ago to determine whether a difference in activity could be measured after a simultaneous irradiation of two samples of lead iodide in the HFBR, one sample being shielded by cadmium. The idea for this type of experiment was originally suggested by Finston and Yellin[38] as a means of determining tnccs of many reactor-produced radionuclides. The experiment gave a lower limit for the tnccs of I^{126} of 1650 barns.

A. Samples and irradiations

Seven samples of lead iodide were irradiated in the HFBR in 1969. Three of the samples were shielded by 0.100 inches of cadmium. The thermal neutron flux was monitored by Co-Al alloy wire. When the aluminum irradiation thimble was opened in the hot cell facility, it was found that the cadmium shield had melted in several spots during the irradiation. Some photographs of the breakdown of the cadmium shield were taken and are shown in Figure 1. The flux monitors inside the cadmium shield were lost and for only three of the bare samples were flux monitors found. The decay of I^{126} was followed and a halflife, $t_{\frac{1}{2}} = 13.1 \pm 0.3$ days, was determined. Reported values are in the range of 13.1 to 13.3 days. An approximate value for the effective cross section was obtained, assuming (as in the previous experiment) that k=0. The thermal neutron flux was taken to be 1.65×10^{14} $n/cm^2/sec$.[39] The lower limit of the effective cross section for this experiment was determined to be 5000 barns.

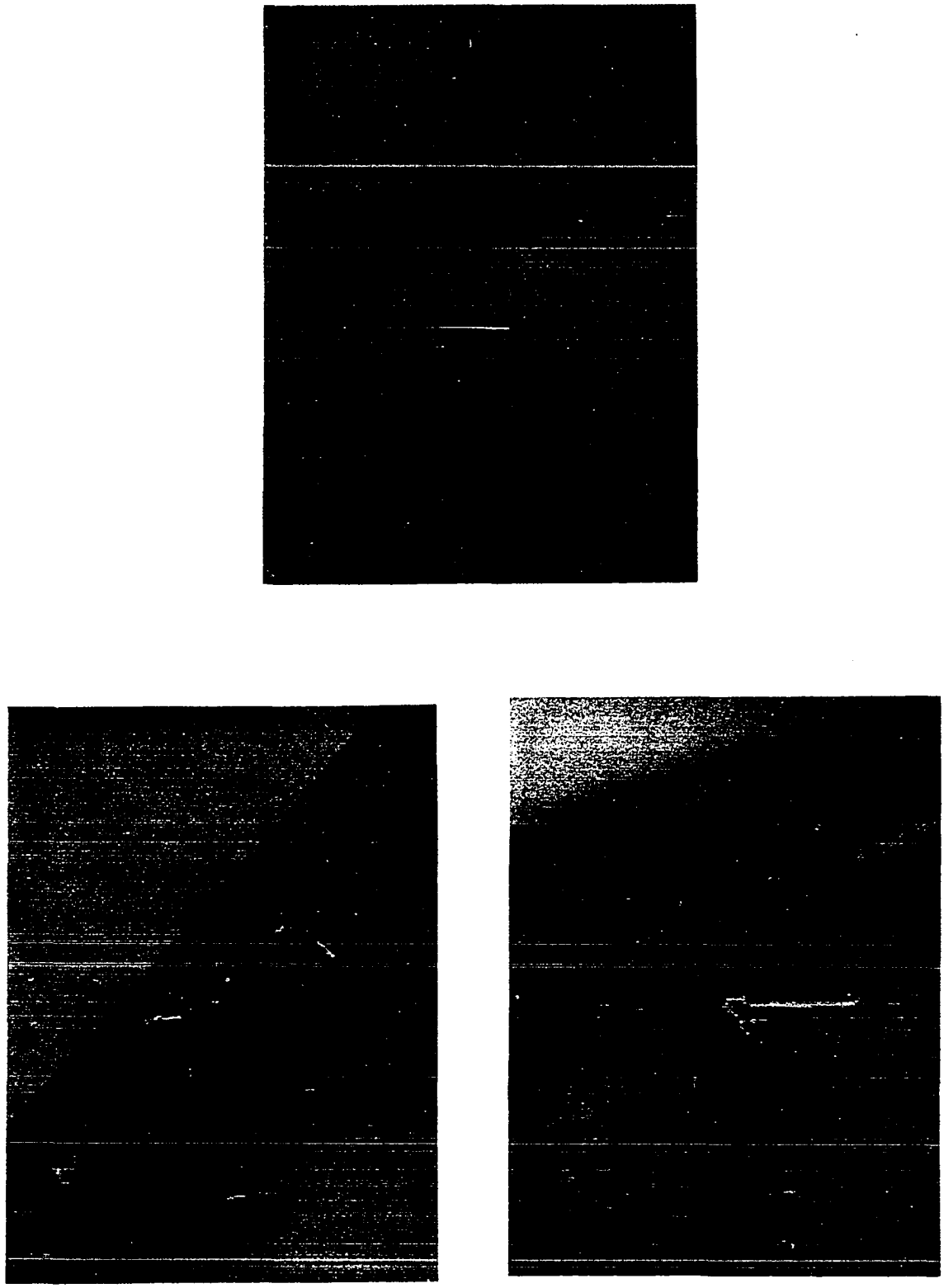

Figure 1. Breakdown of the cadmium shield.

The failure of the cadmium shield, after discussions with Mr. J.J. Floyd at the B.N.L. graphite research reactor, was attributed to the fact that the cadmium shield had made poor thermal contact with the aluminum irradiation thimble, which is cooled by water.

The irradiation thimble was redesigned to prevent the buildup of heat. The thimble was originally designed to hold four samples of lead iodide. The cadmium shield (thickness = 0.050 inches) was force-fit into the aluminum thimble to ensure good thermal contact. Samples of lead iodide (Baker "Analyzed" reagent grade PbI_2) were placed in ampoules of high purity quartz glass and dried at 105°C to constant weight. The ampoules were then sealed. All sealed ampoules were less than one inch in length and less than six millimeters in diameter because of space considerations in the core irradiation position. Flux monitors were obtained from Brookhaven National Laboratory. The thermal flux monitor was 0.015 inch diameter cobalt-aluminum alloy wire, labeled "Bar #6, 0.503% Co-Al". The fast flux monitor was 0.015 inch diameter nickel wire, labeled "BNL C 37552, CP Ni, Bar #7". The ampoules were individually wrapped in aluminum foil. Each foil packet contained a lead iodide ampoule, a thermal flux monitor, and a fast flux monitor.

We were informed, one week before the irradiation was to take place, that twice the space originally planned for would be made available for this experiment. Therefore, four samples of sodium carbonate, certified A.C.S. reagent grade Na_2CO_3,

anhydrous (Fisher Scientific Co.), were dried to constant weight at 180°C, sealed in quartz ampoules, and packaged (as previously described) in aluminum foil. These samples are reserved for another investigation ($t_{\frac{1}{2}}$= 2.3 yr).

The radioactive nuclides whose tnccs were to be determined in this experiment were I^{126} ($t_{\frac{1}{2}}$= 13.1 d, produced by $I^{127}(n,2n)I^{126}$), Sb^{124} ($t_{\frac{1}{2}}$= 61.3 d, produced by $I^{127}(n,\alpha)Sb^{124}$), and Co^{58} ($t_{\frac{1}{2}}$=71.3 d, produced by $Ni^{58}(n,p)Co^{58}$).

The samples of lead iodide and sodium carbonate were delivered to Mr. J.J. Floyd at Brookhaven National Laboratory, where they were placed in the aluminum irradiation thimble. The machinist's diagram for this thimble is shown in Figure II. The cadmium sleeve was capped at both ends with cadmium covers, and the thimble was sealed by welding.

The thimble was placed in the V-16 irradiation facility, which is one of the two in-core irradiation positions of the HFBR, on March 28, 1970. The HFBR was started up on March 31 at 2:15 PM and shut down on April 21 at 1:15 AM. The irradiation thimble was opened in a hot cell on May 15. The ampoules and flux monitors were found to be physically intact, and were delivered to Brooklyn College at the end of June, 1970.

B. Gamma ray spectroscopy

A diagram of the counting system used is shown in Figure III. A listing of the components follows:

1. Ge(Li) detector: This solid-state detector was obtained from Princeton Gamma-Tech, Inc. The detector was kept

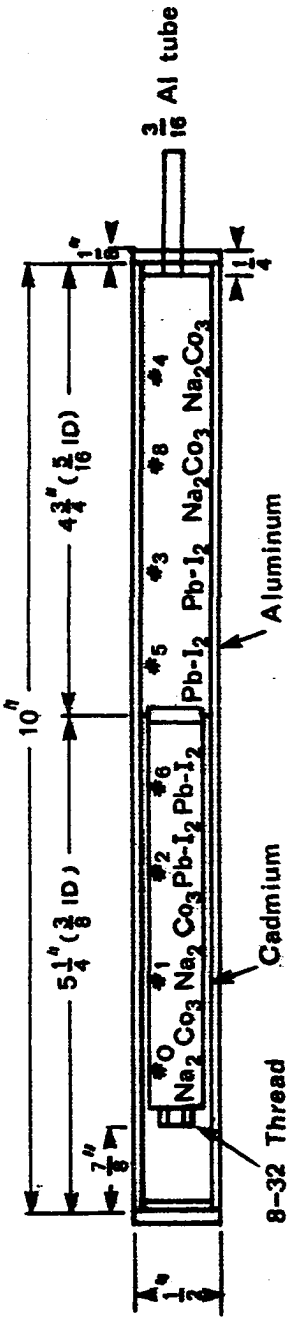

Figure 11. The irradiation thimble.

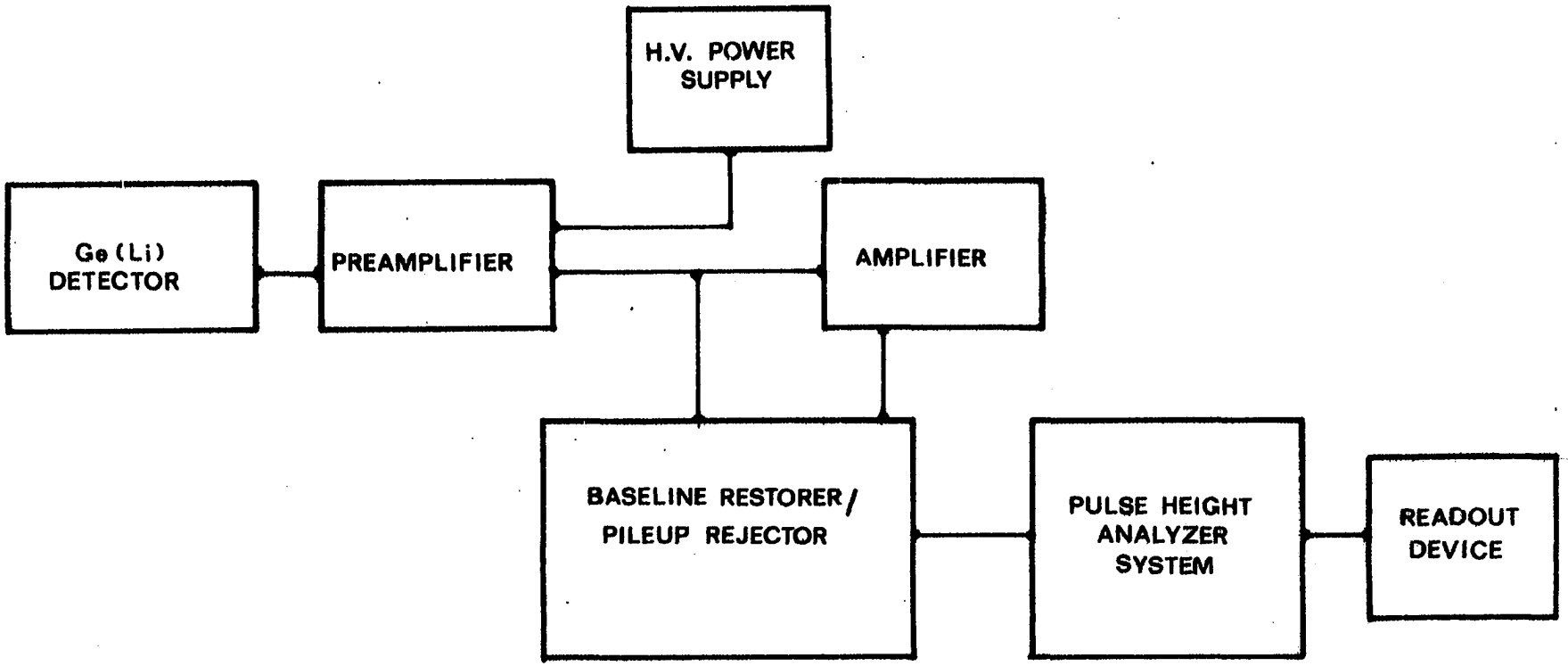

Figure III. The counting system.

at liquid nitrogen temperature at all times.

2. Preamplifier: The Canberra model 1408C charge-sensitive (FET input) spectroscopy preamplifier is an all silicon transistor device which integrates the charge output signals from a cooled Ge(Li) detector for presentation to a pulse shaping main amplifier.

3. Amplifier: The amplifier used was a Canberra model 1417 spectroscopy amplifier, which was selected for its highly stable linear design (better than $\pm$0.075% linearity), extremely low noise contribution, and near-optimum Gaussian pulse shaping.

4. Baseline restorer/Pileup rejector: This unit was a Canberra model 1464 baseline restorer/pileup rejector. This module alleviates the major problems of high count rate, high resolution spectroscopy, namely baseline fluctuations, low frequency noise enhancement (due to Pole/Zero compensation), and pulse pileup.

5. Pulse height analyzer system: The system used was manufactured by Northern Scientific Co. It consisted of a NS-627 ADC/Stabilizer and NS-630 Memory Unit. The address available in the ADC was thirteen bits (conversion gain = 8192). This unit also contained a digital stabilizer which kept zero level and conversion gain at fixed positions, thereby keeping the gain of the entire system constant at all times. The memory unit is capable of storing a twelve bit address (4096 channels).

There is a maximum of 10^6 - 1 counts stored per address before overflow occurs.

6. Readout device: Three readout systems were routinely used. Spectra were recorded on magnetic tape using a NS-406 readout unit, NS-406M magnetic tape interface, and and Ampex TMZ-1 magnetic tape unit. The spectra were printed out on paper using a Franklin (series 1200) high-speed digital printer. Spectra were also recorded on an Omnigraphic (series 2100-3-3) X-Y recorder, manufactured by Houston Instruments.

An Ortec (model 419) precision pulse generator and a Tetronix (type 453) oscilloscope were used routinely to check the electronics. Wang desk-top calculators (Models 360 and 380) were used for routine mathematical calculations. All computer analyses were done with the IBM 360/40 computer at Brooklyn College.

An example of the spectrum of a lead iodide sample from 0.3 MeV to 0.7 MeV taken in July, 1970 is shown in Figure IV.

C. Computer analysis of spectra

An available linear least-squares program for the analysis of gamma ray peaks was modified and used to determine the peak position, FWHM, and area of (experimental) gamma ray peaks. A listing of the program can be found in Appendix I. The program fits the experimental gamma ray peak to a skewed Gaussian curve (which better represents the actual peak obtained with a Ge(Li) detector) by the method of least-squares. The function used for the skewed Gaussian curve was

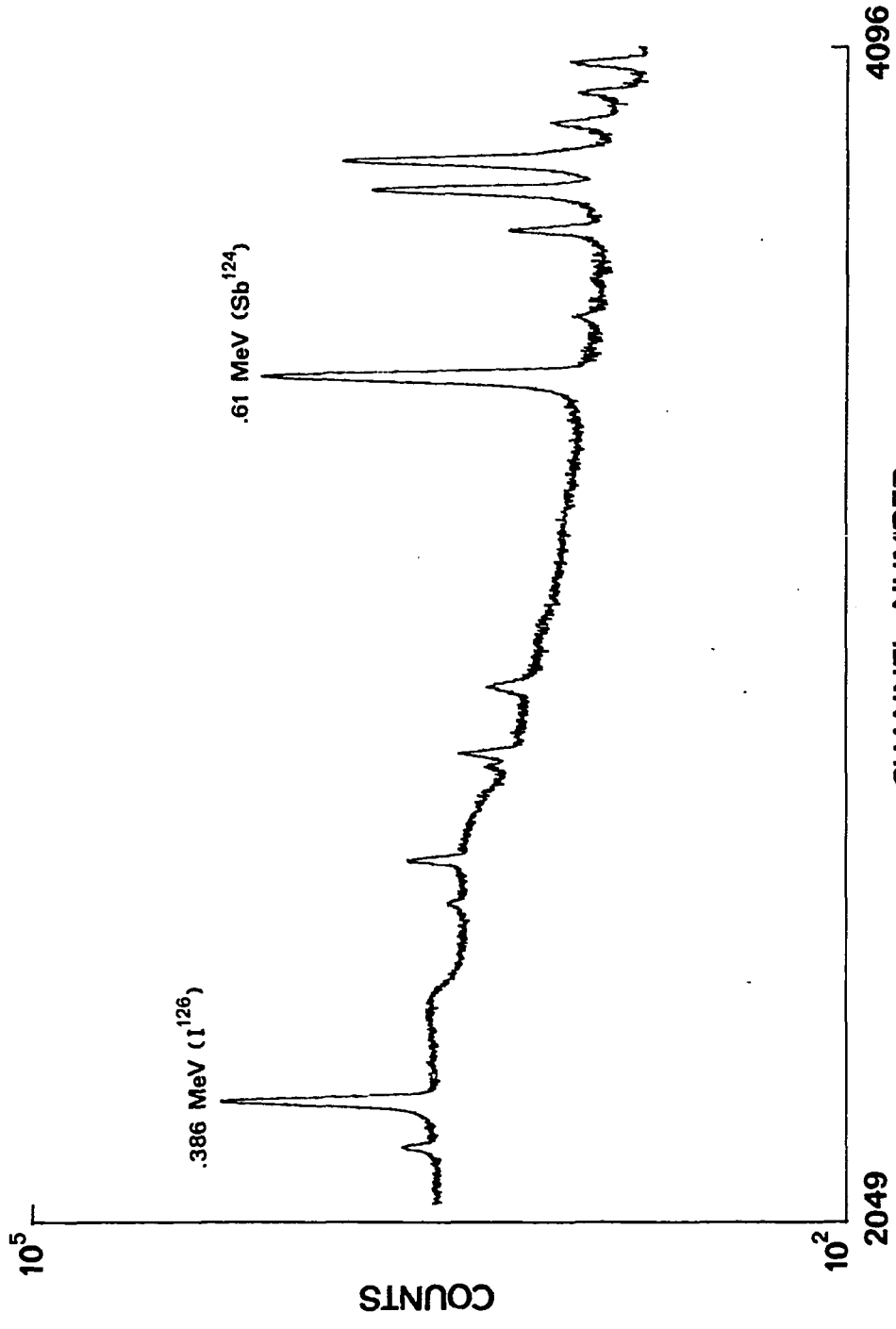

Figure IV. Spectrum of PbI_2, sample #5, July 25, 1970.

$$y = \alpha_1 e^{[-(x - \alpha_2)^2/\alpha_3^2]} + \alpha_4 x + \alpha_5 \qquad (51)$$

where: α_1 = peak height

α_2 = peak centroid

α_3 = FWHM

α_4 = slope of the background

α_5 = y-intercept of the background.

An example of the results obtained by this method of analysis is shown in Figure V. The data used were the 0.386 MeV peak of lead iodide, sample #6, taken on July 31, 1970. The deviation (95% confidence level) of the area was $\pm$ 0.88%, which was a typical value for the error in the fit of the skewed Gaussian curve to the experimental data.

Subsequently, a change in amplification was made, so that spectra of the various nuclides could be obtained without having to change amplification, and to observe the complete spectrum for each nuclide. However, the computer program is somewhat sensitive to the number of channels chosen to encompass the peak of interest. Therefore, the effect of the change in amplification on the analysis of the 0.386 MeV peak for I^{126} was obtained by comparing the areas of the peak under both amplifications. In July, forty points were used to encompass this peak. With the change in amplification, only twenty-two points were used to encompass the peak. As a result of these measurements, experimental data obtained under the old conditions of amplification were multiplied by the factor 1.038 for I^{126}. An example of the spectrum obtained under the new conditions is shown in

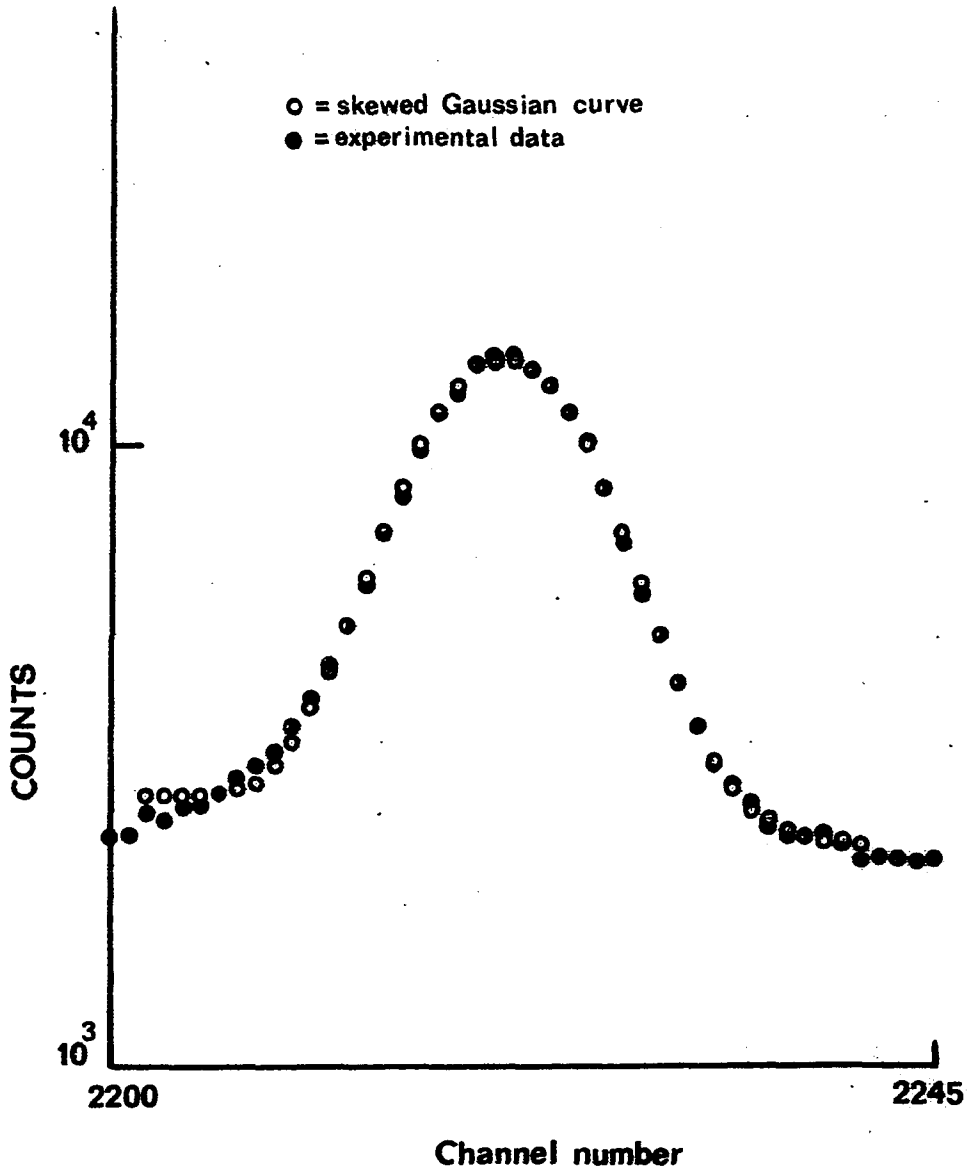

Figure V. Computer analysis of experimental data.

Figure VI for lead iodide. An expanded part of this spectrum is shown in Figure VII for comparison with the spectrum under the old amplification.

A typical spectrum for Co^{60} is shown in Figure VIII. The new amplification settings were equivalent to a value of 0.341 KeV per channel. The full-width at half-maximum for the 1.33 MeV peak of Co^{60} was typically about 2.62 KeV at this amplification.

A typical spectrum obtained for Co^{58} (from the $Ni^{58}(n,p)Co^{58}$ reaction of the fast flux monitor) is shown in Figure IX. The higher energy portion of this spectrum indicated the presence of Co^{60}, which would result from successive neutron captures by Co^{58} and Co^{59}.

It has often been the practice in determining the activity of a given radionuclide in an activated sample to count a broad region of the spectrum. Due to the intense flux of neutrons and the long irradiation time, however, a number of other activities may be produced which would interfere. The high resolving power of the Ge(Li) detector allows one to count individual gamma ray peaks in the spectrum. The decay schemes of each nuclide are well known and each has a conveniently prominent gamma ray. Since the method depends on a relative measurement, it is necessary to know neither the absolute intensity of the gamma ray nor the fraction of decays giving rise to the gamma ray. The 0.386 MeV gamma ray was used for all analyses of I^{126} activity. The 0.603 MeV gamma ray in the same spectrum was used for the analysis of Sb^{124} activity. For Co^{58}, the 0.810 MeV gamma ray

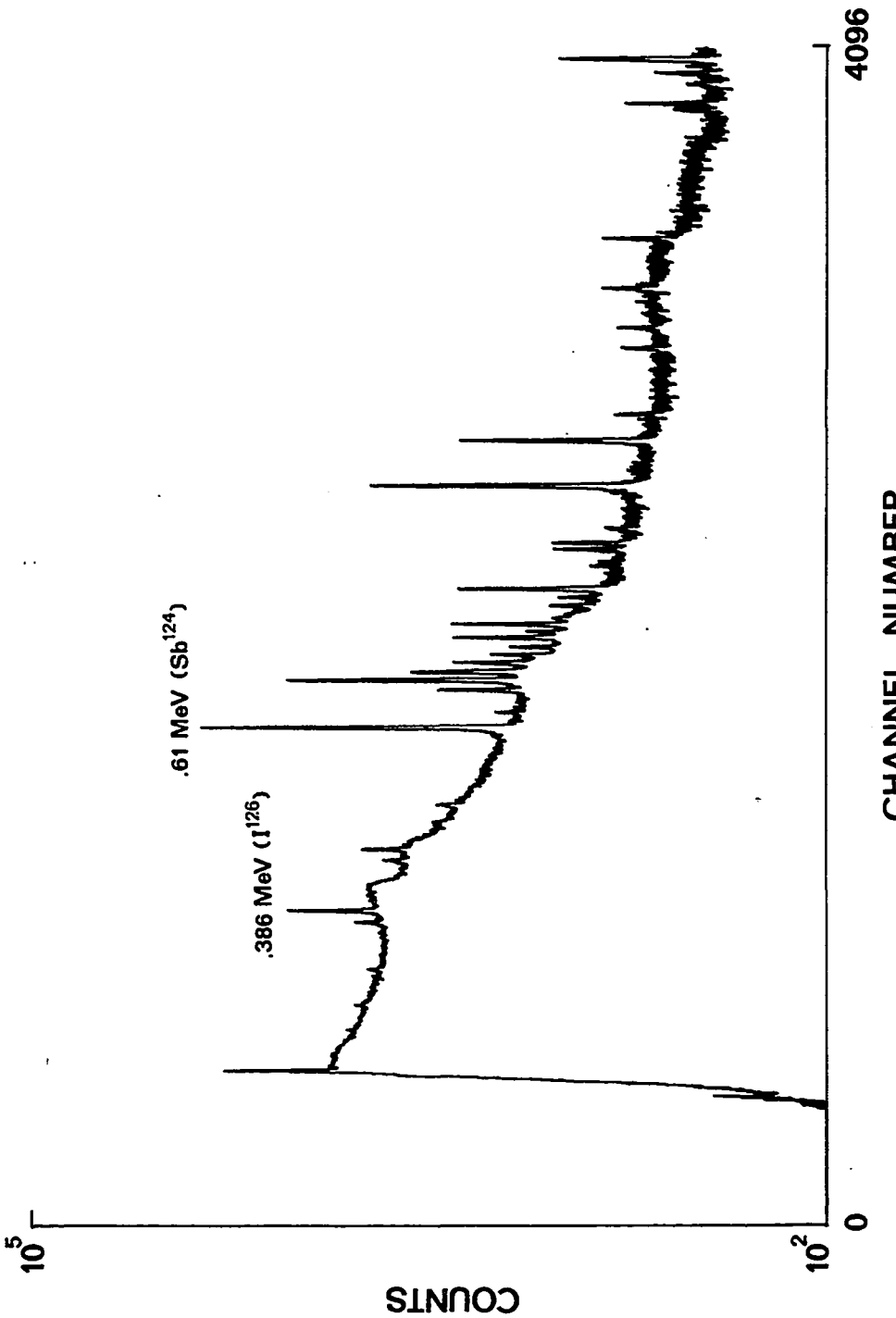

Figure VI. Spectrum of PbI_2, sample #5, August 25, 1970.

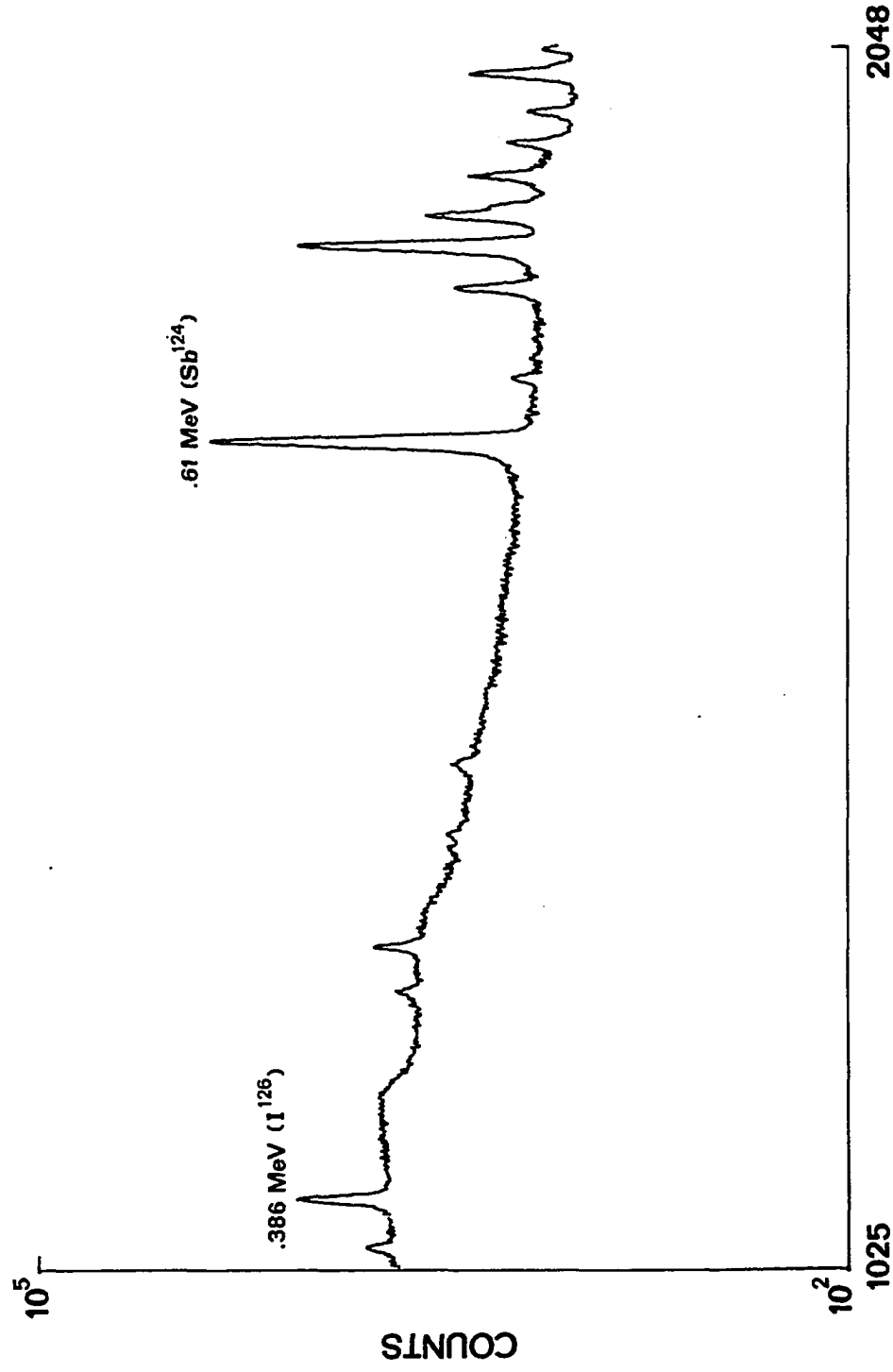

Figure VII. Spectrum of PbI_2, sample #5, August 25, 1970.
Second quarter of Figure VI.

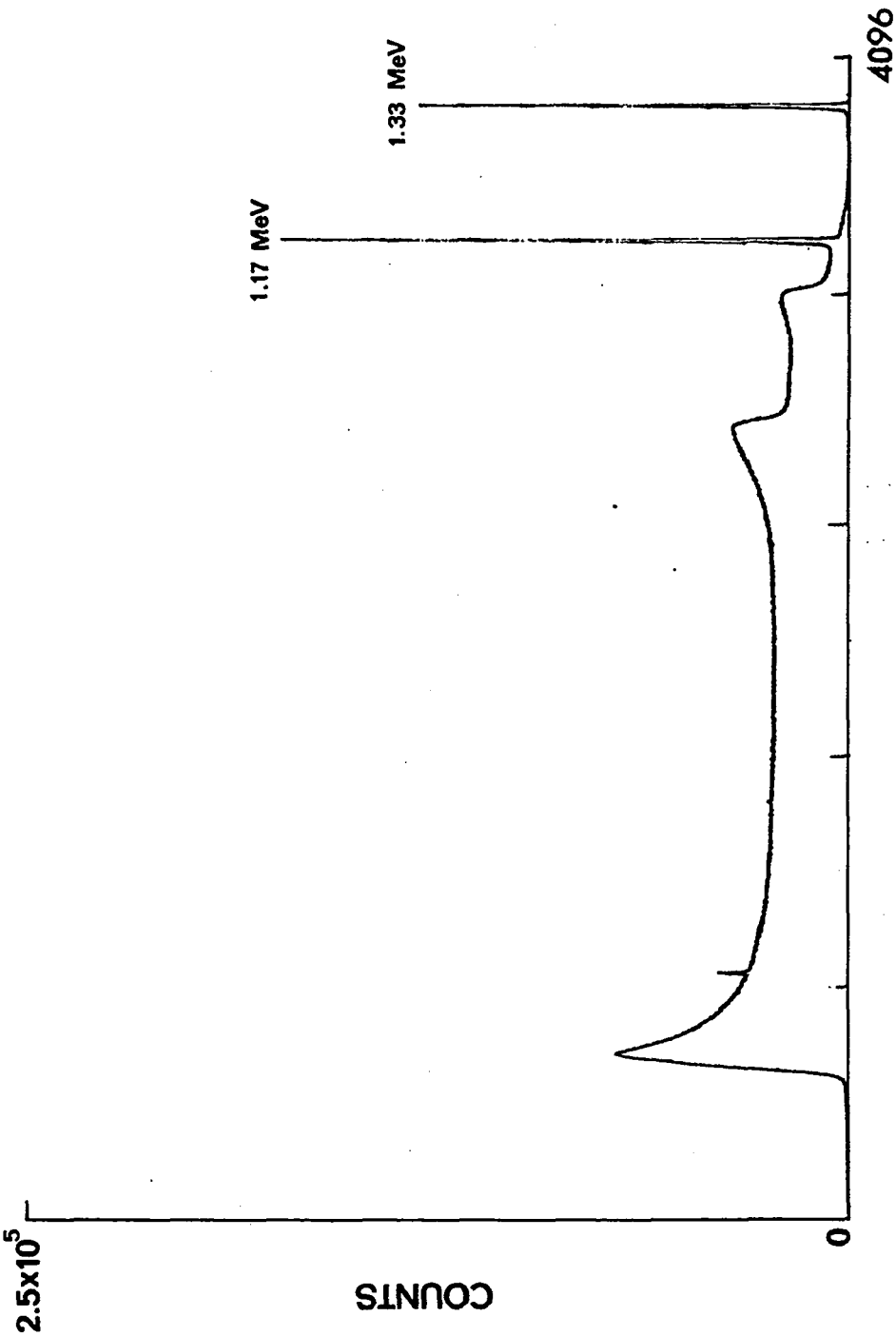

Figure VIII. Spectrum of Co^{60}.

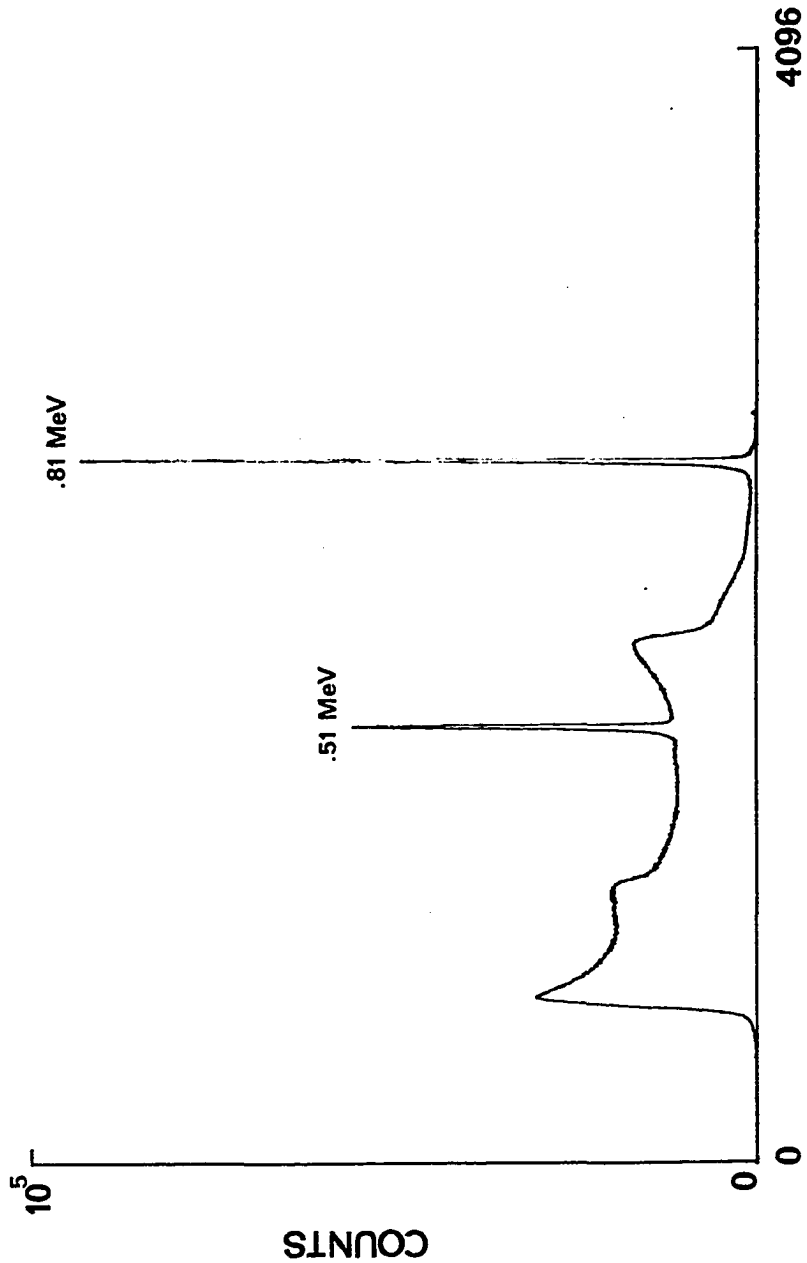

Figure IX. Spectrum of Co^{58}.

was used, and the 1.33 MeV gamma ray was used for the analysis of Co^{60} activity.

D. Treatment of data

Lead iodide and Co^{58} samples were counted for a period of 3000 seconds. The Co^{60} samples were counted for various periods of time, up to a maximum of 10^5 seconds. The change in activity over the counting interval was less than 0.09% for I^{126}, and less than 0.02% for Sb^{124}, Co^{58} and Co^{60}.

The remarkable stability of the system amplification simplified the computer analysis of the data considerably. The centroid of a peak was found to shift no more than $\pm$ 0.5 channels over the period of investigation. Since the position of a particular peak was essentially constant, comparisons of data from day to day were valid.

The decay of I^{126} was followed for a period of five halflives (i.e. about two months). The decay curves for the four samples are shown in Figure X. The halflife was obtained in each case by a least-squares analysis of the experimental data. The average of the four determinations, $t_{\frac{1}{2}} = 13.1 \pm 0.2$ days, was used to determine the decay constant used for all calculations involving I^{126}. The activity of each sample of I^{126} at the end of the irradiation in the HFBR (the y-intercept) was obtained by fitting each set of experimental data to a decay curve of $t_{\frac{1}{2}} = 13.1$ days. The results of these calculations were used to obtain the ratio N_{Cd}/N_B for I^{126}, where the relationship

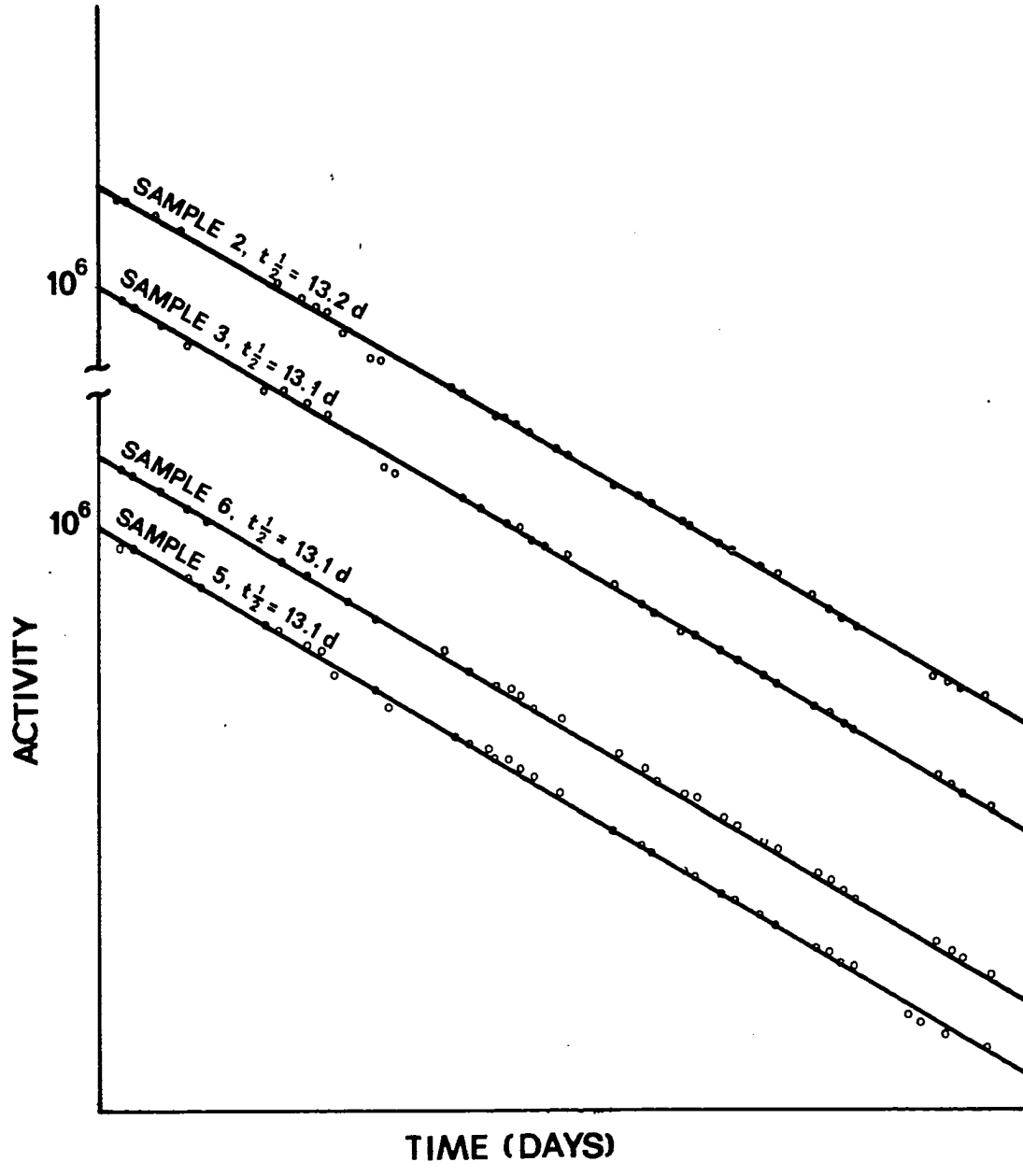

Figure X. Decay curves for I^{126}.

$$\frac{N_{Cd}}{N_B} = \frac{A_{Cd}}{A_B} \tag{52}$$

was used.

Ratios for Sb^{124}, Co^{58}, and Co^{60} were obtained by averaging the results of individual measurements taken over a period of five months. The halflives used for these nuclides were obtained from the literature, since they are too long for experimental verification in a period of less than a year.

A spectrum obtained from sodium carbonate is shown in Figure XI. The complexity of the spectrum indicated that the chemical used was impure. Since the contaminants were unknown, it was decided to allow the sodium samples to decay, in the hope that the longest-lived component would be Na^{22} ($t_{\frac{1}{2}}$= 2.3 years). A spectrum of sodium carbonate taken on January 25, 1971 is shown in Figure XII. Comparison of this spectrum with the previous spectrum (Figure XI) indicates that results may yet be obtained for the tnccs of Na^{22} from this irradiation. The spectrum obtained from a standard sample of Na^{22} is shown in Figure XIII for reference.

The data obtained from the computer analysis of the spectra were used to obtain N_{Cd}/N_B, and this ratio was used for the calculation of the effective cross section. Equation (39) was rearranged to give

$$\frac{A_{Cd}(\lambda + k\hat{\sigma}nv_o)}{A_B(\lambda + \hat{\sigma}nv_o)} - \frac{1 - e^{-[\lambda + k\hat{\sigma}nv_o]t}}{1 - e^{-[\lambda + \hat{\sigma}nv_o]t}} = 0 . \tag{53}$$

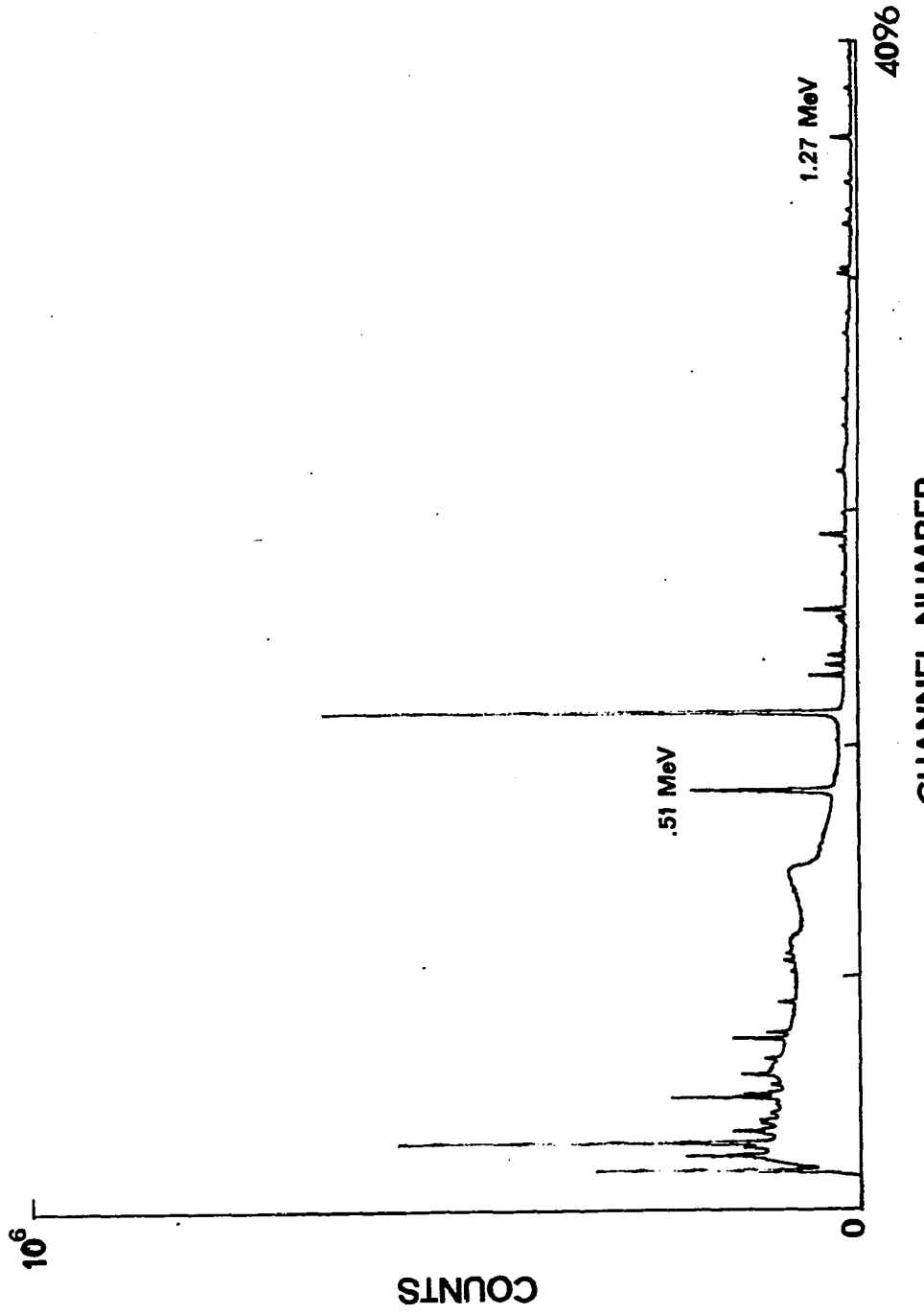

Figure XI. Spectrum of Na_2CO_3, August 17, 1970.

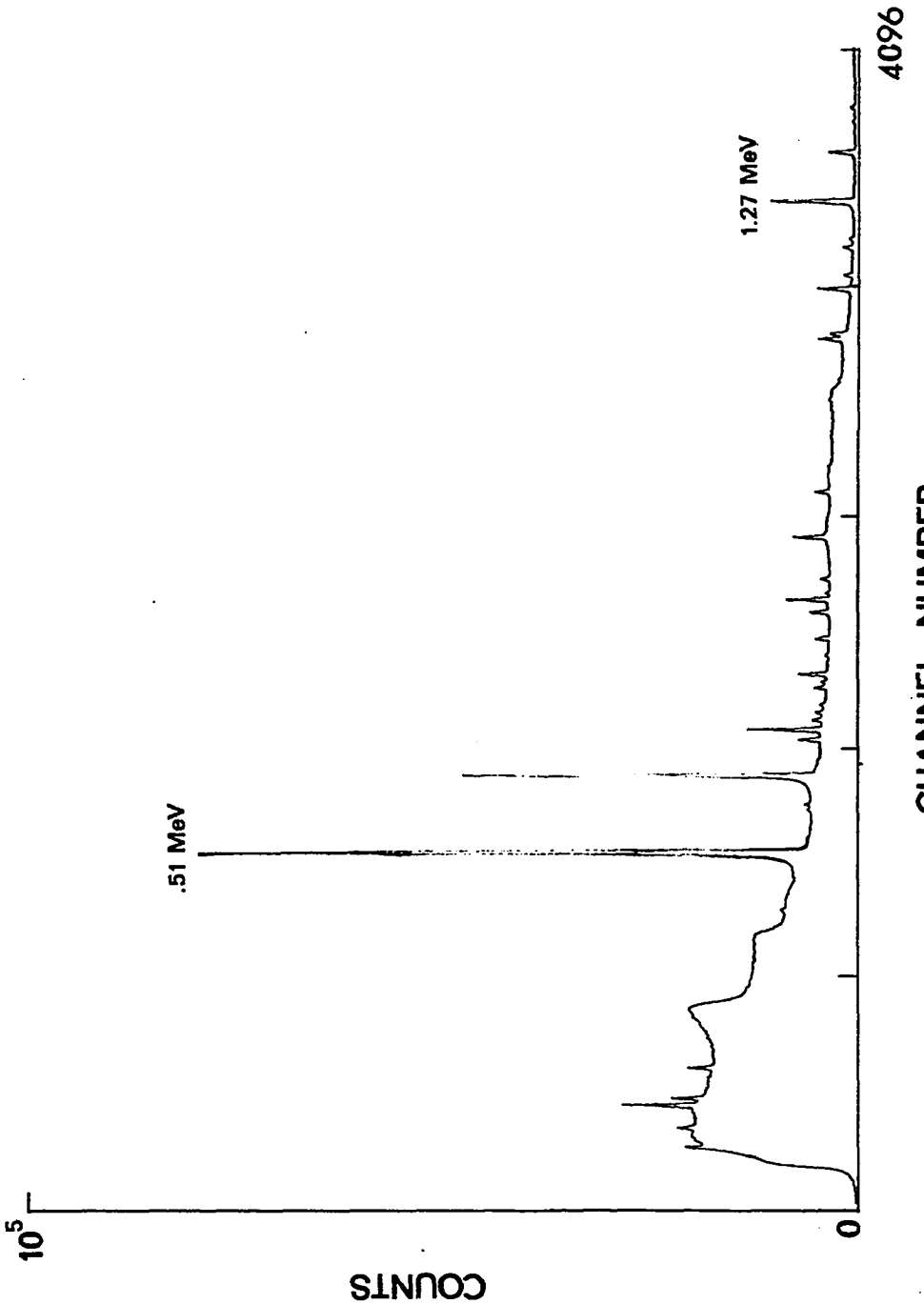

Figure XII. Spectrum of Na_2CO_3, January 25, 1971.

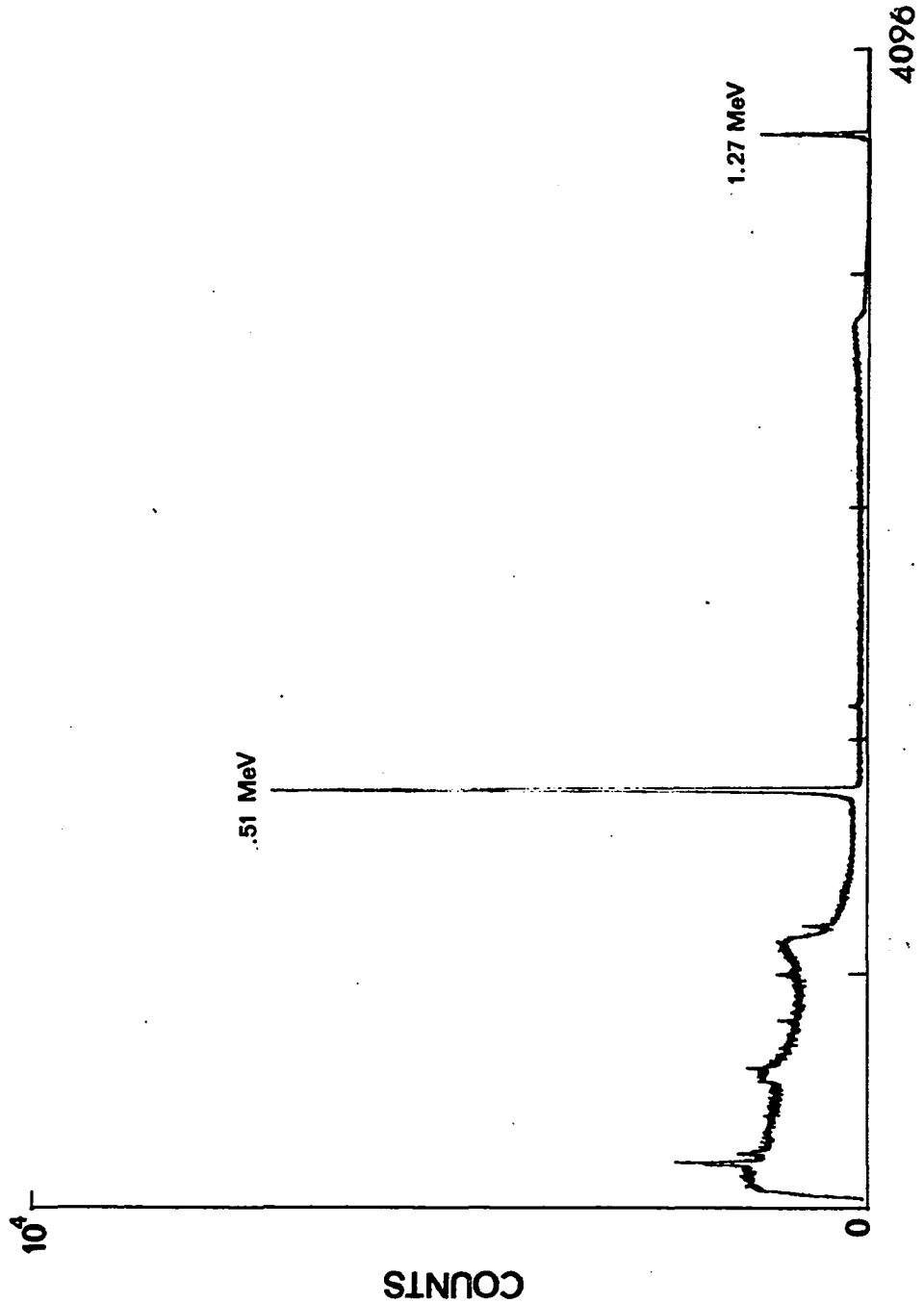

Figure XIII. Spectrum of standard Na^{22}.

Trial functions for σnv_o were used to evaluate this equation numerically. The program used for these calculations is shown in Appendix II. The value of A_{Cd}/A_B used for each nuclide was the average of all experimental values, after correction for decay using the relationship

$$A_o = Ae^{\lambda t} \tag{54}$$

where: A_o = activity at the end of irradiation

A = observed activity

λ = decay constant for the nuclide

t = time from the end of irradiation to time of observed activity.

IV. Results and Discussion

A. Results

The data obtained from the thermal flux monitors (activity of Co^{60}) were used to obtain nv_o by following the Westcott formalism. Equation (53) was solved numerically for I^{126}, Sb^{124} and Co^{58} to obtain the effective cross section (σ) for these nuclides. The procedure developed in Chapter II, section D was followed to obtain the Westcott parameters for these nuclides. The results of these calculations are shown in Table I.

B. Errors

All flux measurements were based on comparison to a calibrated NBS Standard Co^{60} source. The weighing of the cobalt-aluminum alloy flux wires (4mg) introduced an error of ± 2.5% (all errors are stated for the 95% confidence level). The deviation of nine calculated average N_{Cd}/N_B ratios for Co^{60} was ± 2%.

The error in the determination of the activities for I^{126}, Sb^{124} and Co^{58} was taken to be the deviation of the skewed Gaussian curve from the experimental points. This error was calculated to be ± 1.5% for I^{126}, ± 2% for Sb^{124}, and ± 3% for Co^{58}.

The error of the ratio N_{Cd}/N_B for I^{126} was ± 1.5% arising from the least-squares fit of the experimental points to the average halflife decay curve. The uncertainty of the ratio N_{Cd}/N_B for Sb^{124} and Co^{58} was determined to be ± 2% for both nuclides. The uncertainty of the weight of the nickel fast flux monitors (20 mg) was 0.5%.

Table I. Westcott parameters for Co^{60}, I^{126}, Sb^{124} and Co^{58}.

Westcott parameter	Co^{60}	I^{126}	Sb^{124}	Co^{58}
R (bare)	8.74×10^{-9}	---	---	---
N_{Cd}/N_B	---	1.77	1.41	1.30
R_{Cd}	2.14	1.34	1.68	1.78
$r(T/T_o)^{\frac{1}{2}}$	0.347	0.347	0.347	0.347
s_o	1.736	6.79	3.18	2.72
nv_o (bare)	1.46×10^{14}	1.46×10^{14}	1.46×10^{14}	1.46×10^{14}
$\hat{\sigma}$ (barns)	59.8	2.00×10^{4}	6.29×10^{3}	4.48×10^{3}
σ_o (barns)	37.3	5.96×10^{3}	2.99×10^{3}	2.31×10^{3}
Resonance Integral (barns)	76.1	4.06×10^{4}	1.02×10^{4}	6.89×10^{3}

The total deviation of each nuclide was taken to be the sum of the individual errors. The results are compared to other reported values in Table II.

C. Discussion

Comparison of the values reported in Table II shows them to be in reasonable agreement (when appropriate) with previously reported values. The results for I^{126} indicates that this method can be applied for investigations of many radioactive nuclides for which there are no reported values of Westcott parameters. The simplicity of this technique and the fact that all measurements are relative lead us to believe that more reliable results can be obtained than by conventional burnup techniques.

The results for Co^{58} should be studied very carefully since the $Ni^{58}(n,p)Co^{58}$ reaction is used as a primary standard for the determination of the fast neutron flux. Thus, the fast neutron cross sections of many nuclides have been based on this reaction. Although the Westcott σ_o for Co^{58} differs somewhat from previously reported work, the significant difference for the value of the resonance integral should be noted. If the Co^{58} resonance integral was zero, the effective cross section, $\hat{\sigma}$, is just the 2200 m/sec cross section, σ_o, in any neutron flux. All correction factors (reference (32)) for the burnup of Co^{58} (taking into account the length of irradiation and the thermal neutron flux) have been based on this observation. The fact that, in this work, there is a value for the resonance integral of Co^{58}, i.e. $\hat{\sigma} \neq \sigma_o$, means that, unless the thermal neutron flux is known (and R_{Cd} for cobalt

Table II. Final data for I^{126}, Sb^{124} and Co^{58}.

Nuclide	This Work (barns)	Other Work (barns)
I^{126}	$\hat{\sigma} = 20000 \pm 1500$	no reported value
	$\sigma_o = 5960 \pm 450$	no reported value
	RI = 40600 ± 3050	no reported value
Sb^{124}	$\hat{\sigma} = 6290 \pm 540$	no reported value
	$\sigma_o = 2990 \pm 260$	20[29], 2000[30]
	RI = 10200 ± 870	no reported value
Co^{58}	$\hat{\sigma} = 4480 \pm 450$	no reported value
	$\sigma_o = 2310 \pm 230$	1650[32], 3750[33]
	RI = 6890 ± 690	Zero[32]

can be deduced), it would be impossible to determine the fast neutron flux using nickel monitors. Thus, in view of our results, many of the fast neutron cross sections reported for nuclides are not valid. It was assumed in the calculation of the effective cross section that the production of Co^{58} was independent of the thermal neutron flux. Therefore, the production of Co^{58} in bare and cadmium-covered samples was considered to be equal. Previously reported results[32] for Co^{58} indicated that this assumption might not be valid for this nuclide. The complete scheme for the production, burnup and decay of this nuclide is shown in Figure XIV. Pertinent data for this nuclide have been taken from reference (32).

The reported values for Co^{58m}, σ_o = 140000 barns and the RI = 550000 barns, indicated that the burnup of Co^{58m} would change the relative production rates of Co^{58} in the bare and cadmium-covered samples. The decay of the metastable state would produce 33.7% of the final Co^{58} activity if there were no burnup. Burnup would reduce the amount of Co^{58} produced by decay of the metastable state by a factor equal to

$$\frac{\lambda}{\lambda + \sigma n v_o} . \qquad (55)$$

The N_{Cd}/N_B ratio can now be corrected for the change in production and a new set of Westcott parameters obtained for Co^{58}. The results for different values of σ assumed for Co^{58m} are shown in Table III.

Examination of Table III indicates that neglect of the effect on production rate of burnup results in values of σ_o which are too high. However, it should be noted that the cross section

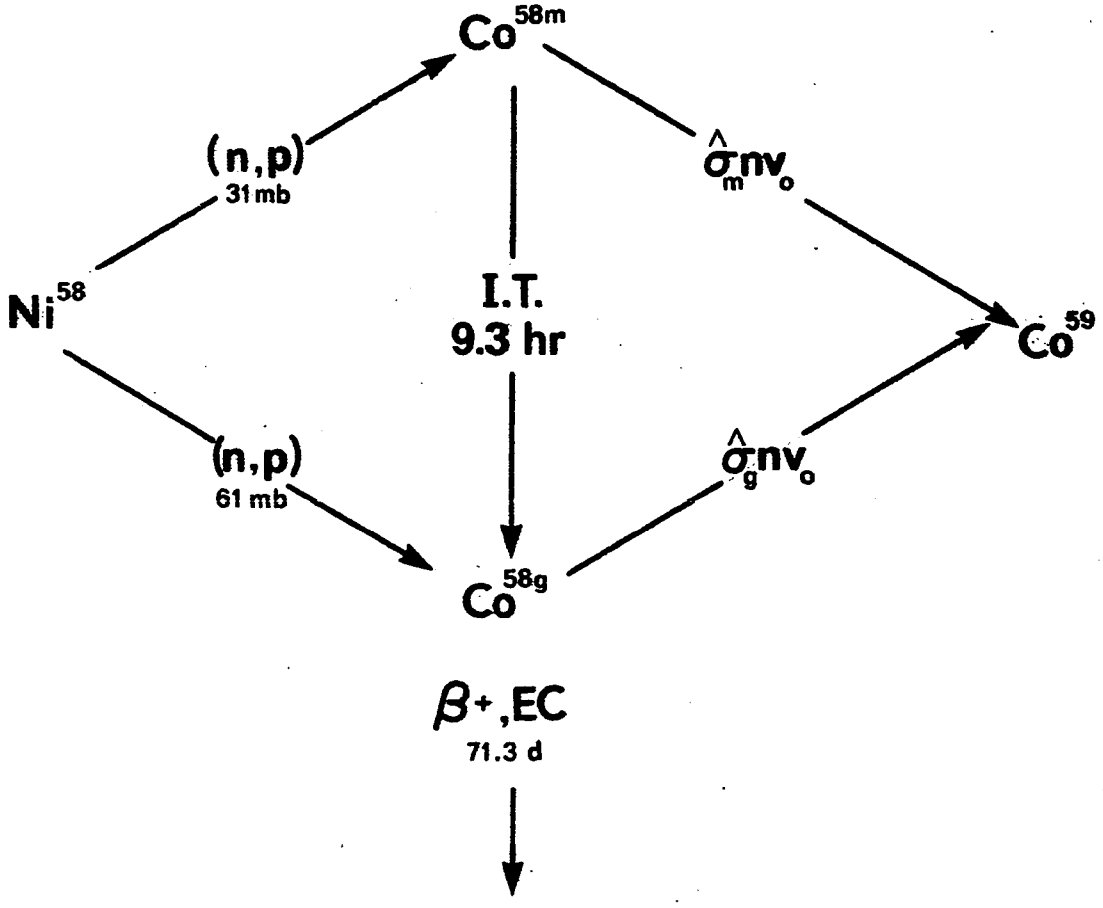

Figure XIV. The reaction scheme for $Ni^{58}(n,p)Co^{58}$.

Table III. Effect of $\hat{\sigma}$ for Co^{58m} on the Westcott parameters for Co^{58}.

Westcott parameter	Trial A	Trial B	Trial C
σ_o (barns), Co^{58m}	1.4×10^5 (32)	1.4×10^4	1.4×10^3
RI (barns), Co^{58m}	5.5×10^5 (32)	5.5×10^4	5.5×10^3
$\hat{\sigma}$ (barns), Co^{58m}	4.5×10^5	4.5×10^4	4.5×10^3
N_B production, Co^{58}	1.12	1.39	(a)
N_{Cd} production, Co^{58}	1.20	1.44	(a)
N_{Cd}/N_B, Co^{58}	1.21	1.25	(1.30)
R_{Cd}, Co^{58}	1.28	1.57	(1.78)
s_o, Co^{58}	8.24	3.86	(2.72)
$\hat{\sigma}$ (barns), Co^{58}	3.06×10^3	3.64×10^3	(4.48×10^3)
σ_o (barns), Co^{58}	8.00×10^2	1.56×10^3	(2.31×10^3)
RI (barns), Co^{58}	6.50×10^3	6.30×10^3	(6.89×10^3)

(a) The results for this trial function indicated that the effect of Co^{58m} burnup on the production of the ground state isomer was negligible. Therefore, the experimental results (from Table I) have been listed, in parentheses, for purposes of comparison.

for the metastable state must be a very large value for this effect to be seen.

Proper use of this new analytical technique would enable one to solve for the Westcott parameters of the Co^{58m}- Co^{58g} problem. An irradiation under two different thicknesses of cadmium should provide sufficient information to determine the two cross sections if the approximate value for one of the effective cross sections is known. This type of irradiation would also provide an excellent method of determining the reliability of the Westcott formalism.

It would be of some interest to irradiate target nuclides under shields of elements other than cadmium, i.e. indium, which would screen out other portions of the neutron spectrum. These irradiations might provide information on the resonance portion of the cross section which is not directly obtained when using cadmium.

The method described provides a simple experimental technique for obtaining many cross sections previously considered too difficult (experimentally) to obtain and for verifying values reported using other techniques. The method may prove to be readily adaptable to other neutron sources, such as Cockroft-Walton accelerators. It would be interesting to see whether or not results for cross sections could be obtained for Co^{58m} or F^{18} by applying this technique to irradiations with Cockroft-Walton accelerators or similar neutron sources.

Appendix I. Computer program for the least-squares fit of a modified Gaussian function to experimental gamma ray spectra.

MAIN PROGRAM

```
C       LEAST SQUARES IN N LINEAR UNKNOWNS
        DIMENSION ERR(10)
        DIMENSION WT(100),ALP(10),FUNT(100),FMT(100),Z(10),BMAT(10,21)
        DIMENSION AALP(10),ERROR(10),XXC(10,12),DUM1(1000),X(100),
       1Y(100)
        DIMENSION Q(96)
        COMMON XXC,DUM1,X,Y,WT,ALP,FUNT,FMT,Z,DETPP,BMAT
        EXTRA=EXP(1.0)
 9898   READ (1,798) MUNK,NITER,KB,KE,KRUN
        IF(MUNK)802,803,802
  803   STOP
  802   FKB=KB
        NPTS=KE-KB+1
        READ (1,799)(ALP(I), I=1,MUNK)
        READ (1,799) (ERR(I), I=1,MUNK)
        READ (1,1002) (Y(I), I=1,NPTS)
 1002   FORMAT(7F10.0)
        WRITE(3,1001) (Y(I), I=1,NPTS)
 1001   FORMAT(1H ,10F10.1)
        X(1)=FKB
        DO 809 I=2,NPTS
  809   X(I)=X(I-1)+1.0
        WRITE (3,810) KRUN,NPTS
  810   FORMAT(1H1,1X,6HRUN NO,I7,3X,6HNO PTS,I7)
  798   FORMAT(2I3,2I4,I3)
  799   FORMAT(7F10.0)
        FNPTS=NPTS
        FMUNK=MUNK
        NIT=0
  559   CALL ALPTT(NPTS,NIT,MUNK)
        CALL COET(MUNK,NPTS,1)
        CALL DETTR(0,MUNK,0)
        DEL=DETPP
        IF(DEL)5554,5555,5554
 5554   DO 554 I=1,MUNK
  554   AALP(I)=ALP(I)+Z(I)
        DO 555 I=1,MUNK
        IF(ABS(AALP(I)-ALP(I))-ERR(I))555,555,557
  555   CONTINUE
        GO TO 588
  557   NIT=NIT+1
        WRITE (3,75) NIT
   75   FORMAT(1X,7HITER NO,I4)
        DO 458 I=1,MUNK
        ALP(I)=AALP(I)
  458   WRITE (3,795) I,ALP(I)
        IF(NIT-NITER)559,559,560
  588   DO 461 I=1,MUNK
  461   ALP(I)=AALP(I)
```

```
      CALL ALPTT(NPTS,NIT,MUNK)
      STAN=0.0
      DO 589 I=1,NPTS
  589 STAN=WT(I)*FMT(I)*FMT(I)+STAN
      STAND=ABS(STAN/(FNPTS-FMUNK))
      IF(STAND-1.0)591,592,592
  591 STAND=1.0
  592 AREA=ALP(1)*ALP(3)*1.7724539
      CALL COET(MUNK,NPTS,1)
      CALL DETTR(0,MUNK,1)
      DO 1 I=1,MUNK
      DO 2 J=1,MUNK
      BMAT(I,J)=BMAT(I,J)*STAND
      IF(I-J)2,4,2
    4 ERROR(I)=SQRT(ABS(BMAT(I,I)))
    2 CONTINUE
    1 CONTINUE
      FWHM=ALP(3)*2.0*SQRT(ALOG(2.0))
      FWHE=ABS(ERROR(3)*2.0*SQRT(ALOG(2.0)))
      ARER=(ALP(1)*ERROR(3))**2+(ALP(3)*ERROR(1))**2
      ARER=1.7724539*SQRT(ABS(ARER+2.*ALP(1)*ALP(3)*BMAT(1,3)))
      DO 695 I=1,MUNK
  695 WRITE(3,692) I,ALP(I),ERROR(I)
      IF(MUNK-6)6,5,8
    5 WRITE(3,699)((BMAT(I,J),J=1,MUNK),I=1,MUNK)
  699 FORMAT(//1H ,6E20.8)
      GO TO 705
    6 WRITE(3,700)((BMAT(I,J),I=1,MUNK),J=1,MUNK)
  700 FORMAT(//1H ,5E20.8)
      GO TO 705
    8 WRITE(3,711)((BMAT(I,J),I=1,MUNK),J=1,MUNK)
  711 FORMAT(//1H ,7E17.8)
  705 WRITE(3,702)STAN
  702 FORMAT(1H ,7HCHI SQ#,E18.8)
      WRITE (3,698)AREA,ARER,FWHM,FWHE
  698 FORMAT(6H AREA#E18.8,5X,3HSD#E18.8,5X,5HFWHM#E18.8,5X,3HSD#E18.8)
      WRITE(3,797)
  797 FORMAT(1H ,5X,1HX,19X,4HYFIT,16X,2HYD,18X,14HABS%Y-YFIT</YD)
      DO 796 J=1,NPTS
      YD=SQRT(Y(J))
      SD=ABS(FMT(J)/YD)
      WRITE(3,498)J,X(J),Y(J),FUNT(J),YD,SD
  498 FORMAT(1H ,I3,5(E16.8,4X))
  796 CONTINUE
      GO TO 9898
 5555 WRITE(3,110)
  110 FORMAT(14H DEPENDENT EQS/12H DATA SKIPPD)
      DO 691 I=1,NPTS
  691 WRITE (3,692) I,X(I),Y(I)
  692 FORMAT(1XI4,2E18.8)
      GO TO 9898
  560 WRITE(3,693)
```

```
693 FORMAT(20H TOO MANY ITERATIONS)
    DO 694 I=1,MUNK
694 WRITE (3,795)I,ALP(I)
795 FORMAT(1X13,E18.8)
    GO TO 9898
    END
```

SUBROUTINE ALPTT

```
    SUBROUTINE ALPTT(KPTS,KTIME,MUNK)
    DIMENSION DUM2(10,12),A(100,10),XC(100),YC(100),WW(100),ALPH(10)
    DIMENSION FUN(100),FM(100)
    COMMON DUM2,A,XC,YC,WW,ALPH,FUN,FM
    IF (KTIME)1,2,1
  2 DO 3 I=1,KPTS
    IF(MUNK-6)5,6,9
  5 A(I,4)=XC(I)
    A(I,5)=1.0
    GO TO 3
  6 A(I,5)=XC(I)
    A(I,6)=1.0
    A(I,4)=XC(I)**2
    GO TO 3
  9 A(I,6)=XC(I)
    A(I,4)=XC(I)**3
    A(I,5)=XC(I)**2
    A(I,7)=1.0
  3 WW(I)=1.0/YC(I)
  1 ALP3=ALPH(3)*ALPH(3)
    DO 4 I=1,KPTS
    XMAL2=XC(I)-ALPH(2)
    A(I,1)=EXP(-XMAL2*XMAL2/ALP3)
    A(I,2)=2.0*ALPH(1)*A(I,1)*XMAL2/ALP3
    A(I,3)=A(I,2)*XMAL2/ALPH(3)
    IF(MUNK-6)7,8,10
  7 FUN(I)=ALPH(1)*A(I,1)+ALPH(4)*XC(I)+ALPH(5)
    GO TO 4
  8 FUN(I)=ALPH(1)*A(I,1)+ALPH(4)*A(I,4)+ALPH(5)*XC(I)+ALPH(6)
    GO TO 4
 10 FUN(I)=ALPH(1)*A(I,1)+ALPH(4)*A(I,4)+ALPH(5)*A(I,5)+ALPH(6)*XC(I)
    FUN(I)=FUN(I)+ALPH(7)
  4 FM(I)=YC(I)-FUN(I)
    RETURN
    END
```

SUBROUTINE COET

```
      SUBROUTINE COET(NUNK,NOPTS,KBRN)
      DIMENSION XCOEF(10,12),AA(100,10),D(200),W(100),D2(10)
      DIMENSION FUNK(100),FMM(100)
      COMMON XCOEF,AA,D,W,D2,FUNK,FMM
      KUNK1=NUNK+1
      DO 12 L=1,NUNK
      DO 11 M=1,KUNK1
   11 XCOEF(L,M)=0.0
   12 CONTINUE
      DO 13 L=1,NUNK
      DO 14 M=1,NUNK
      IF(L-M)15,15,16
   16 XCOEF(L,M)=XCOEF(M,L)
      GO TO 14
   15 DO 17 I=1,NOPTS
      GO TO (18,19),KBRN
   18 IF(ABS(AA(I,L))-1.E-65)17,17,221
  221 IF(ABS(AA(I,L))-1.E-32)219,219,220
  219 IF(ABS(AA(I,M))-1.E-32)17,17,218
  220 IF(ABS(AA(I,M))-1.E-65)17,17,218
  218 XCOEF(L,M)=XCOEF(L,M)+W(I)*AA(I,L)*AA(I,M)
      GO TO 17
   19 XCOEF(L,M)=XCOEF(L,M)+AA(I,M)*AA(I,L)/(-FUNK(I))
   17 CONTINUE
   14 CONTINUE
   13 CONTINUE
      GO TO (21,24),KBRN
   21 DO 22 L=1,NUNK
      DO 23 I=1,NOPTS
      IF(ABS(AA(I,L))-1.E-70)23,23,25
   25 XCOEF(L,KUNK1)=XCOEF(L,KUNK1)+W(I)*AA(I,L)*FMM(I)
   23 CONTINUE
   22 CONTINUE
   24 RETURN
      END
```

SUBROUTINE DETTR

```
      SUBROUTINE DETTR(KMIN,LUNK,KERR)
      DIMENSION TEMP(1,21),XCOF(10,12),DUM22(1510),DETM(10),Y(10,21)
      COMMON XCOF,DUM22,DETM,DETMP,Y
      MATC=LUNK
      J=0
```

```
      DO 72 L=1,LUNK
      M=0
      IF(L-KMIN)73,72,73
   73 J=J+1
      DO 74 K=1,LUNK
      IF(K-KMIN)76,74,76
   76 M=M+1
      Y(J,M)=XCOF(L,K)
   74 CONTINUE
   72 CONTINUE
      IF(KMIN)77,78,77
   77 MATR=LUNK-1
      MATC=LUNK
      GO TO 79
   78 MATR=LUNK
      MATC=LUNK+2+KERR*(LUNK-1)
      IF(KERR)80,81,80
   81 DO 82 I=1,MATR
   82 Y(I,MATC-1)=XCOF(I,MATC-1)
      GO TO 79
   80 MATC1=MATC-1
      MATC2=MATC-MATR
      DO 83 L=1,MATR
      DO 84 M=MATC2,MATC1
   84 Y(L,M)=0.0
   83 CONTINUE
      DO 85 L=1,MATR
      MMAM=MATR+L
   85 Y(L,MMAM)=1.0
   79 DO 86 I=1,MATR
   86 Y(I,MATC)=1.0
      DO 212 I=1,MATR
      M=I+1
      J=1
  885 IF(Y(I,I))213,214,213
  214 IF(J-MATR)215,226,215
  215 J=J+1
      DO 216 L=1,MATC
      TEMP(1,L)=Y(I,L)
      Y(I,L)=Y(J,L)
  216 Y(J,L)=TEMP(1,L)
      GO TO 885
  213 IF(I-MATR)281,282,281
  281 YDIV=1.0/Y(I,I)
      DO 220 K=M,MATC
  220 Y(I,K)=Y(I,K)*YDIV
      Y(I,I)=1.0
      DO 221 L=M,MATR
      MATC1=MATC-1
      DO 222 K=M,MATC1
      Y(L,K)=Y(I,K)*(-Y(L,I))+Y(L,K)
```

```
  222 CONTINUE
  221 CONTINUE
      DO 224 L=M,MATR
  224 Y(L,I)=0.0
  212 CONTINUE
  282 MMM=MATR+1
      YDIV=1.0/Y(MATR,MATR)
      DO 899 KK=MMM,MATC
  899 Y(MATR,KK)=Y(MATR,KK)*YDIV
      Y(MATR,MATR)=1.0
      DETMP=1.0
      IF(KERR)851,851,852
  851 DO 825 I=1,MATR
  825 DETMP=DETMP*Y(I,MATC)
      DETMP=1.0/DETMP
      IF(KMIN)46,45,46
   46 RETURN
   45 DETM(MATR)=Y(MATR,MATR+1)
      JO=0
  875 JO=JO+1
      JIP=MATR-JO
      IF(JIP)891,46,891
  891 KIP=JIP+1
      DETM(JIP)=Y(JIP,MATR+1)
      DO 999 L=KIP,MATR
  999 DETM(JIP)=DETM(JIP)-DETM(L)*Y(JIP,L)
      GO TO 875
  852 MATC=MATC-1
      DO 8111 I=2,MATR
      II=I-1
      DO 8112 K=1,II
      III=I+1
      DO 8113 J=III,MATC
 8113 Y(K,J)=-Y(K,I)*Y(I,J)+Y(K,J)
 8112 Y(K,I)=0.0
 8111 CONTINUE
      DO 853 L=1,MATR
      DO 854 M=1,MATR
      MMATR=M+MATR
  854 Y(L,M)=Y(L,MMATR)
  853 CONTINUE
      RETURN
  226 DETMP=0.0
      RETURN
      END
```

Appendix II. Wang program for the numerical solution of equation (53).

STEP	COMMAND	CODE
00	Mark	07
01	1	61
02	Cl A_L	54
03	Cl A_R	50
04	Stop	01
05	Cont	06
06	St Dir	26
07	4	64
08	$+A_L$	56
09	Enter	41
10	Rec Dir	27
11	3	63
12	X=	46
13	$+A_R$	52
14	Rec Dir	27
15	2	62
16	$+A_L$	56
17	Rec Dir	27
18	2	62
19	$+A_R$	52
20	Enter	41
21	Rec Dir	27
22	0	60
23	Enter	41
24	Rec A_L	55
25	$\div=$	47
26	St Dir	26
27	5	65
28	Rec Dir	27
29	1	61
30	Enter	41

STEP	COMMAND	CODE
31	Rec A_L	55
32	X=	46
33	Ch Sign	77
34	e^x	43
35	Cl A_L	54
36	$-A_L$	57
37	Rec Dir	27
38	1	61
39	Enter	41
40	Rec A_R	51
41	X=	46
42	Ch Sign	77
43	e^x	43
44	Cl A_R	50
45	$-A_R$	53
46	1	61
47	$+A_R$	52
48	Enter	41
49	1	61
50	$+A_L$	56
51	$\div=$	47
52	Cl A_L	54
53	$-A_L$	57
54	Rec Dir	27
55	5	65
56	$+A_L$	56
57	Search	02
58	1	61

The program now loops to step 00 and resets.

COMMENTS

a) Store N_{Cd}/N_B in memory 0.
b) Store time of irradiation in memory 1.
c) Store λ in memory 2.
d) Store k in memory 3.
e) Clear all and Search 1.
f) Punch out a trial numerical value for $\hat{\sigma}nv_o$ on the keyboard.
g) Press continue.
The value for the expression in equation (53) is displayed at the end of the program. If the sign is positive, the trial function chosen was too great. Steps f and g are repeated until a minimal value for the expression is obtained. The trial function is stored in memory 4 for reference.

BIBLIOGRAPHY

1. I. Kaplan, "Nuclear Physics", Addison-Wesley Publ. Co., Reading, Mass., 1962, p. 647.

2. G. Friedlander, J.W. Kennedy and J.M. Miller, "Nuclear and Radiochemistry", second edition, John Wiley and Sons, Inc., N.Y., 1964, p. 476.

3. G. Friedlander, J.W. Kennedy and J.M. Miller, op. cit., p. 474.

4. G. Friedlander, J.W. Kennedy and J.M. Miller, op. cit., p. 328.

5. J.A. Petruska, E.A. Melaika and R.H. Tomlinson, Can. J. Phys., 33, 640 (1955).

6. S. Bernstein, M.M. Shapiro, C.P. Stanford, T.E. Stephenson, J.B. Dial, S. Freed, G.W. Parker, A.R. Brosi, G.M. Hebert and T.W. DeWitt, Phys. Rev., 102 (3), 823 (1956).

7. M.S. Freedman, A. Turkevich, R.M. Adams, N. Sugarman, S. Raynor and L.G. Stang, Jr., JINC, 2, 271 (1956).

8. H.R. Fickel and R.H. Tomlinson, Can. J. Phys., 37, 531 (1959).

9. N. Sugarman, Phys. Rev., 75, 1473 (1949).

10. A.P. Baerg, F. Brown and M. Lounsbury, Can. J. Phys., 36, 863 (1958).

11. M.G. Ingram, R.J. Hayden and D.C. Hess, Phys. Rev., 79, 271 (1950).

12. R.E. Lapp, ibid., 71, 745 (1947).

13. W.J. Sturm, ibid., 71, 757 (1947).

14. T.J. Kennett and H.G. Thode, JINC, 5, 253 (1958).

15. J. MacNamara and H.G. Thode, Phys. Rev., 80, 296 (1950).

16. D.J. Hughes and J.A. Harvey, Brookhaven National Laboratory Report BNL-325 (1955). Unpublished results from Chalk River.

17. E.P. Steinberg and L. Glendenin, "International Conference on the Peaceful Uses of Atomic Energy, Geneva 1955", Paper 614, United Nations, N.Y. (1956).

18. J.C. Roy and L.P. Roy, Can. J. Phys., 37, 907 (1959).

19. C.H. Westcott, W.H. Walker and T.K. Alexander, "Proceedings of the 2nd International Conference on the Peaceful Uses of Atomic Energy, Geneva 1958", United Nations, N.Y., 16, p. 70 (1959).

20. Tape and Cork, Phys. Rev., 53, 676 (1938).

21. J.J. Livingood and G.T. Seaborg, ibid., 54, 775 (1938).

22. D.L. Mock, R.C. Waddell, L.W. Fagg and R.A. Tobin, ibid., 74, 1536 (1948).

23. N.L. Perlman and J.P. Welker, ibid., 95, 133 (1954).

24. L. Koerts, P. Macklin, B. Farrelly, R. van Lieshout and C.S. Wu, ibid., 98, 1230 (1955).

25. P.A. Aagaard, G. Andersson, J.O. Burgman and A.C. Pappas, JINC, 5, 105 (1957).

26. G.G. Jonsson and B. Forkman, Nucl. Phys., A 107, 52 (1968).

27. H.C. Roy and D. Wuschke, Can. J. Chem., 36, 1424 (1958).

28. M. Bresesti, A.M. del Turco, H. Neumann and E. Orvini, JINC, 26, 1625 (1964).

29. T.A. Eastwood and F. Brown, PR-CM-36, p. 7 (Chalk River).

30. A.N. Murin, V.D. Nefedov, D.K. Popov and V.I. Baranovsky, Atomnaya Energiya, 2, 553 (1957).

31. D.J. Hughes and R.B. Schwartz, "Neutron Cross Sections", BNL-325, to be published. These cross sections were obtained from Dr. J. Stehn of the National Cross Section Center at Brookhaven National Laboratory.

32. C.H. Hogg, L.D. Weber and E.C. Yates, "Thermal Neutron Cross Sections of the Co^{58} Isomers and the Effect on Fast Flux Measurements Using Nickel", IDO-16744, Idaho Falls (1964).

33. J.M. Davidson and J.W. Helm, General Electric Co., Hanford Atomic Products Operation, Richland, Wash. Contract AF(45-1), p. 1350 (1961).

34. G. Breit and E.P. Wigner, Phys. Rev., 49, 519, 642 (1936).

35. G. Friedlander, J.W. Kennedy and J.M. Miller, op. cit., p. 339.

36. C.C. Trail - private communication.

37. T.A. Eastwood, A.P. Baerg, C.B. Bigham, F. Brown, M.J. Cabell, W.E. Grummitt, J.C. Roy, L.P. Roy and R.P. Schuman, "Proceedings of the 2nd International Conference on the Peaceful

Uses of Atomic Energy, Geneva 1958", United Nations, N.Y., 16, p. 54 (1959).

38. H.L. Finston and E. Yellin - private communication.

39. J.J. Floyd - private communication.

BIOGRAPHICAL NOTE

The author was born in Brooklyn, New York on September 7, 1940. He graduated from New York University in 1963. After some industrial experience, he entered Brooklyn College as a part-time student in 1964. He was admitted to the Doctoral Program in Chemistry in 1967 at the City University of New York.

In December, 1964, the author and Annette Reiss were married. They are expecting their first child in June.

For the coming year, the author is the recipient of an Ames Laboratory Research Post-Doctoral Fellowship at Iowa State University.